ORIGINAL RESEARCH

Natural History of Cardiomyopathy in Adult Dogs With Golden Retriever Muscular Dystrophy

Lee-Jae Guo, DVM, MS; Jonathan H. Soslow, MD; Amanda K. Bettis, BS; Peter P. Nghiem, DVM, PhD; Kevin J. Cummings, DVM, PhD; Mark W. Lenox, PhD; Matthew W. Miller, DVM, MS; Joe N. Kornegay, DVM, PhD; Christopher F. Spurney, MD

***Background*—**Duchenne muscular dystrophy (DMD) is an X-linked disease that causes progressive muscle weakness. Affected boys typically die from respiratory or cardiac failure. Golden retriever muscular dystrophy (GRMD) is genetically homologous with DMD and causes analogous skeletal and cardiac muscle disease. Previous studies have detailed features of GRMD cardiomyopathy in mostly young dogs. Cardiac disease is not well characterized in adult GRMD dogs, and cardiac magnetic resonance (CMR) imaging studies have not been completed.

***Methods and Results*—**We evaluated echocardiography and CMR in 24 adult GRMD dogs at different ages. Left ventricular systolic and diastolic functions, wall thickness, and myocardial strain were assessed with echocardiography. Features evaluated with CMR included left ventricular function, chamber size, myocardial mass, and late gadolinium enhancement. Our results largely paralleled those of DMD cardiomyopathy. Ejection fraction and fractional shortening correlated well with age, with systolic dysfunction occurring at ≈30 to 45 months. Circumferential strain was more sensitive than ejection fraction in early disease detection. Evidence of left ventricular chamber dilatation provided proof of dilated cardiomyopathy. Late gadolinium enhancement imaging showed DMD-like left ventricular lateral wall lesions and earlier involvement of the anterior septum. Multiple functional indexes were graded objectively and added, with and without late gadolinium enhancement, to give cardiac and cardiomyopathy scores of disease severity. Consistent with DMD, there was parallel skeletal muscle involvement, as tibiotarsal joint flexion torque declined in tandem with cardiac function.

***Conclusions*—**This study established parallels of progressive cardiomyopathy between dystrophic dogs and boys, further validating GRMD as a model of DMD cardiac disease. **(*J Am Heart Assoc*. 2019;8:e012443. DOI: 10.1161/JAHA.119.012443.)**

Key Words: cardiac imaging • cardiomyopathy • Duchenne muscular dystrophy • golden retriever muscular dystrophy • natural history

Duchenne muscular dystrophy (DMD) is an X-linked recessive disorder affecting ≈1 of 3500 to 5000 male births. Mutations in the *DMD* (dystrophin) gene lead to loss of dystrophin protein at the muscle cell membrane and progressive loss of appendicular, respiratory, and cardiac muscle function.[1–3] With implementation of more aggressive respiratory supportive care over the past few decades, cardiac failure has supplanted respiratory disease as the major cause of death in DMD. Currently, many patients with DMD die in their third or fourth decade because of progressive cardiomyopathy.[4,5] Although the exact pathogenesis and distribution of cardiac lesions in DMD cardiomyopathy are not completely defined, lesions tend to begin in the left ventricular (LV) posterior basal wall and progress to a dilated cardiomyopathy.[3,6,7] Many therapeutic approaches for DMD have been proposed, with some being assessed in preclinical models or in clinical trials. However, because of the late onset of cardiomyopathy in DMD, the assessment of therapeutic

From the Departments of Veterinary Integrative Biosciences (L.-J.G., A.K.B., P.P.N., J.N.K.) and Small Animal Clinical Sciences (M.W.M.), and Texas A&M Institute for Preclinical Studies (L.-J.G.), College of Veterinary Medicine and Biomedical Sciences, Texas A&M University, College Station, TX; Division of Pediatric Cardiology, Department of Pediatrics, Vanderbilt University Medical Center, Nashville, TN (J.H.S.); Department of Population Medicine and Diagnostic Sciences, College of Veterinary Medicine, Cornell University, Ithaca, NY (K.J.C.); Department of Biomedical Engineering, College of Engineering, Texas A&M University, College Station, TX (M.W.L.); Division of Cardiology and Center for Genetic Medicine Research, Children's National Health System, Washington, DC (C.F.S.).

Accompanying Data S1 and Tables S1 through S4 are available at https://www.ahajournals.org/doi/suppl/10.1161/JAHA.119.012443

Correspondence to: Christopher F. Spurney, MD, 111 Michigan Avenue NW, Washington, DC 20010. E-mail: cspurney@childrensnational.org

Received February 22, 2019; accepted June 26, 2019.

Clinical Perspective

What Is New?

- This natural history study demonstrates that systolic dysfunction occurs at 30 to 45 months in golden retriever muscular dystrophy (GRMD) dogs, and circumferential strain is sensitive in early disease detection.
- Regions of late gadolinium enhancement in GRMD were identified and corresponded to those of Duchenne muscular dystrophy, with evidence of earlier involvement of the anterior septum in GRMD.
- A multiparametric cardiac scoring system was developed to provide a standardized index of disease severity regardless of age, and tibiotarsal joint tetanic flexion torque was progressively lost in tandem with a decline of cardiac function, establishing a relationship between skeletal and cardiac muscle.

What Are the Clinical Implications?

- The natural history of GRMD cardiomyopathy largely parallels that of patients with Duchenne muscular dystrophy, further validating GRMD as a preclinical model for therapeutic studies.
- The multiparametric cardiac and cardiomyopathy scores allow our findings to be extrapolated to GRMD colonies worldwide and to facilitate preclinical therapeutic testing.

benefits and complications remains challenging.[8] To better understand the cardiac effects of potential new therapies, further studies in animal models are needed.[9,10]

Genetically homologous conditions of DMD have been characterized in mice, rats, dogs, and other animal species.[11–16] The 2 main animal models for DMD are *mdx* mice and golden retriever muscular dystrophy (GRMD) dogs. Whereas *mdx* mice develop a relatively mild form of cardiomyopathy,[17] GRMD dogs have a late-onset and more severe form of dilated cardiomyopathy,[18,19] similar to that in people.[20,21] Several studies, mostly limited to young dogs, described characteristics of GRMD cardiomyopathy using different methodologies, including pathology, electrocardiography, and echocardiography.[18,19,22–24] However, given the limited number of dogs evaluated in these studies and the inherent phenotypic variation of GRMD, the natural history of cardiomyopathy in dystrophic dogs remains poorly defined. Moreover, advanced imaging techniques like cardiac magnetic resonance (CMR) have rarely been assessed in GRMD dogs. Accordingly, no clear consensus has been reached on preclinical imaging markers to track disease progression.

The goal of this study was to define the timeline of disease progression and appropriate disease markers of GRMD cardiomyopathy by assessing echocardiography and CMR in a group of adult dystrophic dogs.

Materials and Methods

The data, analytic methods, and study materials will be made available to other researchers for scientific purposes on reasonable request sent to the corresponding author.

All dogs in this study were cared for and assessed according to principles outlined in the National Research Council's Guide for the Care and Use of Laboratory Animals. Studies were approved by the institutional animal care and use committees at the University of North Carolina at Chapel Hill and Texas A&M University.

Study Animals

The study included a total of 24 GRMD dogs from a colony at the University of North Carolina at Chapel Hill that was subsequently moved to Texas A&M University. The GRMD genotype was suspected based on elevated serum creatine kinase and confirmed by genotyping, as described previously.[10,25] Dogs ranged from 9 to 86 months in age. Both hemizygous male (n=15) and homozygous female (n=9) affected dogs were studied. Based on our previous skeletal muscle function data[26] and some preliminary unpublished cardiac results, hemizygous male and homozygous female dogs have a similar phenotype of the disease. Accordingly, data in this study were not assessed separately based on sex.

All imaging data were collected from 2012 to 2016 and then assessed retrospectively. Two echocardiography studies were performed, one at a single time point and another at 2 ages 12 months apart. In a third study, dogs were studied with CMR at a single time point. Imaging modalities varied among dogs, so animal numbers differed across the 3 studies (Figure 1).

Echocardiography

Single-time-point study

Dogs were assessed by echocardiography without sedation. GE Vivid 9 (GE Healthcare) and Siemens Antares (Siemens Medical Solutions USA) ultrasound machines were used. Dogs were transported and rested in the imaging room at least 10 minutes before the scans and then were gently restrained in a lateral recumbent position. Scans were performed in a quiet environment to limit stress artifact. Standard canine echocardiographic scans were performed for 2-dimensional B-mode, M-mode, Doppler flow, and tissue Doppler imaging. Right parasternal short- and long-axis views, left apical 4- and 5-chamber views, and a subxiphoid view were recorded for further analyses. All scans from the GE Vivid 9 were imported to a GE EchoPAC workstation (GE Healthcare) for image analysis. Scans from the Siemens Antares were analyzed directly on the machine. M-mode analysis was performed in

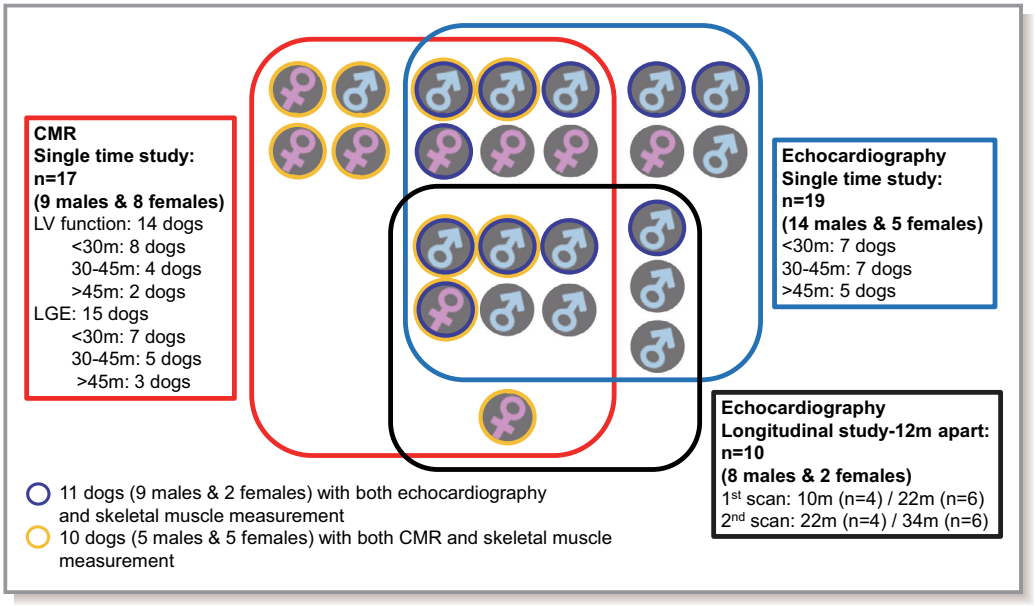

Figure 1. Groups of golden retriever muscular dystrophy dogs for different imaging procedures and techniques. CMR indicates cardiac magnetic resonance imaging; LV, left ventricle; LGE, late gadolinium enhancement.

the right parasternal short-axis view at the level of the papillary muscles to measure wall thickness, chamber diameter, and fractional shortening (FS). M-mode results were normalized for the dog's body mass (kg)[27] to evaluate LV chamber size and myocardial wall thickness (Data S1). LV end-diastolic volume (LVEDV), LV end-systolic volume (LVESV), and ejection fraction (EF) were measured from the right parasternal long-axis view using the modified Simpson rule.[28] Mitral valve E and A wave velocities were measured from the left apical 4-chamber view using pulsed-wave Doppler at the level of the mitral valve tips. Maximal velocity at the aortic valve was measured from the subxiphoid or left apical 5-chamber view using pulsed- or continuous-wave Doppler. The left atrial/aortic root ratio was measured from the right parasternal short-axis basal view using Rishniw and Erb's method.[29] Tissue Doppler imaging was performed at the lateral and septal mitral annulus in the apical 4-chamber view to measure the myocardial systolic and diastolic velocities during the cardiac cycle. Isovolumic relaxation time was measured from the subxiphoid view using continuous-wave Doppler or measured from tissue Doppler imaging. The mid-LV short-axis view, at the level of the papillary muscles, was used for speckle tracking to measure average and segmental circumferential strain and strain rate. All echocardiographic parameters were calculated from an average of 3 to 5 cardiac cycles. To ensure data consistency and accuracy, the speckle-tracking measurements of circumferential strain and strain rate were obtained only from the GE Vivid 9 machine.

Longitudinal study

A separate study assessed dogs with echocardiography at 2 time points, 12 months apart, using a protocol similar to the one described. Scans were all performed on the Siemens Antares ultrasound machine and then imported into Siemens Syngo Velocity Vector Imaging software (Siemens Medical Solutions) for analysis. Average and segmental circumferential strain and strain rate, as well as EF, were measured and then used for comparison.

CMR Imaging

Dogs were premedicated intramuscularly with atropine sulfate (0.04 mg/kg) followed by acepromazine maleate (0.02 mg/kg) and butorphanol tartrate (0.4 mg/kg), masked with sevoflurane (4–5%) to allow intubation, and then maintained under anesthesia with sevoflurane (2–3%) during the scanning period. Premedications were avoided during induction in dogs with signs of congestive heart failure. All CMR scans were performed on a 3-T magnetic resonance imaging machine (Siemens 3T Magnetom Verio; Siemens Medical Solutions) with dogs in a dorsal recumbent position. A cardiac dedicated surface coil was used with ECG or pulse-oximetry gating systems. Breath hold or a free breathing sequence was selected based on the dog's anesthetic status. Three long-axis (2-, 4-, and 3-chamber) views and a series of short-axis views, from the LV base to apex, were scanned using FLASH (fast low-angle shot) imaging or TrueFISP (true fast imaging with steady-state free precession) sequences to generate the cine images. Late gadolinium enhancement (LGE) imaging was performed 10 minutes after injecting 0.2 mmol/kg gadolinium intravenously. The 2- and 4-chamber long-axis and LV short-axis views were collected using a phase-sensitive inversion recovery sequence for LGE imaging.

All CMR images were imported to a Siemens Syngo workstation (Siemens Medical Solutions) for further analysis. LV short-axis cine views were selected for LV functional analysis. The 4-chamber view was used to define the LV basal level for short-axis slices. End-diastolic and end-systolic stages in the cardiac cycle were identified from the short-axis views. Regions of interest were manually drawn by following the endocardial and epicardial edges in all short-axis views at the end-diastolic and end-systolic stages. LVEDV, LVESV, stroke volume, EF, and myocardial mass at end-diastole were analyzed using Siemens Argus software (Siemens Medical Solutions). To obtain the indexed values, CMR data were normalized for body surface area (BSA), calculated from body mass using a standard canine BSA equation[30]: BSA in $m^2=10.1\times(\text{weight in g})^{2/3}/10\ 000$.

Semiquantitative analysis of LGE

A semiquantitative method was developed to assess LGE lesions in CMR. We identified 16 myocardial segments from the short-axis LGE images by modifying American Heart Association standards for myocardial segmentation.[31] The apex was excluded because of imaging overlap between the apex and sternum. The degree of LGE in the 16 myocardial segments was scored from 0 to 2 (Data S1) to indicate enhancement levels ranging from none (dark and black, 0) to either intermediate (gray, 1) or marked (bright and white, 2). Higher scores indicated segments were more enhanced by gadolinium, suggesting extracellular matrix expansion secondary to myocardial fibrosis. The LGE scores and myocardial segments were used for further analysis.

Statistical Analysis

Statistical analysis was performed using JMP Pro 12 software. For the single-time-point study, dogs were divided into 3 age groups (<30, 30 to 45, and >45 months), and relevant values were compared using the Kruskal–Wallis test. If significance was found in the Kruskal–Wallis test, the Dunn test was used to identify the groups that differed significantly. Spearman correlation coefficients were used to assess correlation between age and different echocardiographic and CMR parameters. In the echocardiographic longitudinal study, the Wilcoxon signed rank test was used to compare circumferential strain, strain rate, and EF between the 2 time points. $P<0.05$ was considered statistically significant in all studies.

Results

Animal Groups

Three groups of GRMD dogs were evaluated in different imaging studies (Figure 1). Nineteen dogs (14 male, 5 female) aged 17 to 86 months (median: 33 months) were included in the single-time-point echocardiographic study using 2 different ultrasound machines (Table S1). Ten dogs (6 males aged 22 months; 2 males and 2 females aged 10 months) were imaged longitudinally 12 months apart for circumferential strain, strain rate, and EF measurements. Seventeen dogs (9 male, 8 female) aged 9 to 77 months (median: 22 months) were included in the CMR study. Images from 14 dogs (7 male, 7 female) aged 9 to 77 months (median: 22 months) were of sufficient quality to allow LV functional analysis in CMR. Three dogs were excluded because of inappropriate ECG gating or imaging orientation. The degree of LGE was assessed in 15 dogs (8 male, 7 female) aged 17 to 77 months (median: 30 months). Two dogs did not have sufficient LGE quality to allow assessment.

Echocardiographic Findings in Different Age Groups

For the single-time-point study, GRMD dogs were divided into 3 age groups: <30 months (n=7), 30 to 45 months (n=7), and >45 months (n=5; Table S2). LVEDV, LVESV, LV internal diameter in diastole, and LV internal diameter in systole were increased at >45 versus <30 months ($P=0.02$, $P=0.013$, $P=0.013$, and $P=0.008$, respectively). LVEDV was also increased at >45 versus 30 to 45 months ($P=0.04$). To accommodate the differences in the dogs' body sizes, LVEDV, LVESV, and stroke volume were normalized for BSA (Data S1), to obtain the indexed values. LVEDV index (LVEDVI) was higher at >45 versus <30 and 30 to 45 months ($P=0.03$ for both). LVESV index (LVESVI) was higher at >45 versus <30 and 30 to 45 months ($P=0.02$ and $P=0.04$, respectively). Body mass–normalized LV internal diameters in diastole and systole were higher at >45 versus <30 months ($P=0.03$ and $P=0.02$, respectively). EF and FS were decreased at >45 versus <30 months ($P=0.004$ and $P=0.02$, respectively). Mitral valve A wave velocity was increased at >45 versus 30 to 45 months ($P=0.04$), with an associated lower E/A ratio (mitral valve E wave to A wave ratio) ($P=0.03$). The E/Em ratio (ratio of the mitral valve E wave to early diastolic myocardial velocity in tissue Doppler imaging) at the LV lateral wall was higher at >45 versus <30 months ($P=0.02$). The E/Em ratio at the LV septum was higher at both 30 to 45 and >45 versus <30 months ($P=0.011$ and $P=0.04$).

Correlations Between Echocardiographic Variables and Age

The correlations between echocardiographic variables and age are shown in Table 1. Values that correlated negatively with age, consistent with a decline in systolic function over time, included FS ($\rho=-0.6991$; $P<0.001$), EF ($\rho=-0.7866$; $P<0.001$), and peak systolic myocardial velocity at the LV

Table 1. Correlation Between Age (months) and Echocardiographic and CMR Variables

Variable	Spearman ρ	*P* Value
Echocardiography*		
Heart rate, beats/min	−0.1810	0.46
FS, %	−0.6991	<0.001¶
LA/Ao†	0.5240	0.10
EF, %	−0.7866	<0.001¶
AV V_{max}, m/s	0.1928	0.43
IVRT†, ms	0.6530	0.03§
MV E velocity, m/s	0.2808	0.24
MV A velocity, m/s	0.4250	0.07
E/A ratio	−0.1709	0.48
TDI Em (LV lateral), m/s	−0.4653	0.04§
TDI Am (LV lateral), m/s	0.2904	0.31
TDI Sm (LV lateral), m/s	−0.6813	0.007‖
Em/Am ratio (LV lateral)	−0.5529	0.04§
TDI Em (LV septal), m/s	−0.3539	0.18
TDI Am (LV septal), m/s	0.0897	0.79
TDI Sm (LV septal), m/s	−0.5329	0.09
Em/Am ratio (LV septal)	−0.4055	0.22
E/Em (LV lateral)	0.7062	<0.001¶
E/Em (LV septal)	0.8384	<0.001¶
Circ strain†, average, %	0.7654	0.006‖
Anterior, %	0.4475	0.17
Anteroseptal, %	0.6970	0.02§
Inferoseptal, %	0.4237	0.19
Inferior, %	0.2100	0.54
Inferolateral, %	0.3326	0.32
Anterolateral, %	0.1913	0.57
Circ strain rate†, average, 1/s	0.7244	0.011§
Anterior, 1/s	0.4282	0.19
Anteroseptal, 1/s	0.7973	0.003‖
Inferoseptal, 1/s	0.5148	0.11
Inferior, 1/s	0.6849	0.02§
Inferolateral, 1/s	0.2733	0.42
Anterolateral, 1/s	0.4612	0.15
BSA normalization		
LVEDVI, mL/m^2	0.6359	0.003‖
LVESVI, mL/m^2	0.7203	<0.001¶
SV index, mL/m^2	0.1108	0.65
Body mass normalization		
IVSd-n, cm/kg	0.2219	0.36
LVIDd-n, cm/kg	0.5937	0.007‖
LVPWd-n, cm/kg	0.1591	0.52
IVSs-n, cm/kg	−0.1347	0.58
LVIDs-n, cm/kg	0.6690	0.0017‖
LVPWs-n, cm/kg	0.0757	0.76
LA-n†, cm/kg	0.4920	0.12
Ao-n†, cm/kg	−0.2970	0.38
CMR‡		
Heart rate, beats/min	−0.4175	0.1375
EF, %	−0.7766	0.0011‖
BSA normalization		
LVEDVI, mL/m^2	0.7567	0.0017‖
LVESVI, mL/m^2	0.7146	0.004‖
SV index, mL/m^2	−0.2987	0.30
Myo mass index, g/m^2	0.7412	0.002‖

Am indicates late diastolic myocardial velocity; Ao-n indicates normalized aortic diameter; AV V_{max}, maximal velocity at aortic valve; BSA, body surface area; Circ, circumferential; CMR, cardiac magnetic resonance; E/A ratio, ratio of mitral valve E wave to A wave; E/Em, ratio of the mitral valve E wave to early diastolic myocardial velocity in tissue Doppler imaging; EF, ejection fraction; Em, early diastolic myocardial velocity; FS, fractional shortening; IVRT, isovolumic relaxation time; IVSd-n, normalized interventricular septum in diastole; IVSs-n, normalized interventricular septum in systole; LA/Ao, left atrial to aortic root ratio; LA-n, normalized left atrial diameter; LV lateral, left ventricular lateral wall; LV septal, left ventricular septal wall; LVEDVI, left ventricular end-diastolic volume index; LVESVI, left ventricular end-systolic volume index; LVIDd-n, normalized left ventricular internal diameter in diastole; LVIDs-n, normalized left ventricular internal diameter in systole; LVPWd-n, normalized left ventricular posterior wall in diastole; LVPWs-n, normalized left ventricular posterior wall in systole; MV A, mitral valve A wave; MV E, mitral valve E wave; myo, myocardial; Sm, systolic myocardial velocity; SV, stroke volume; TDI, tissue Doppler imaging.

*Nineteen dogs in a single-time-point echocardiographic study were included for analysis.

†The LA, Ao, IVRT, and strain analytic results were collected only from the 11 dogs using the GE Vivid 9 ultrasound machine.

‡Fourteen dogs in a single-time-point CMR study were included for analysis.

§$P<0.05$.

‖$P<0.01$.

¶$P<0.001$.

lateral wall in tissue Doppler imaging (ρ=−0.6813; *P*=0.007). Average circumferential strain and circumferential strain rate worsened (values became less negative) in older dogs, resulting in a positive correlation with age (ρ=0.7654 and ρ=0.7244; *P*=0.006 and *P*=0.011). With additional segmental strain analysis, there was a positive correlation between age versus circumferential strain and strain rate of the anteroseptal segment (ρ=0.6970 and ρ=0.7973; *P*=0.02 and *P*=0.003). The circumferential strain rate of the inferior segment also showed positive correlation with age (ρ=0.6849; *P*=0.02). LVEDVI, LVESVI, and normalized LV internal diameters in diastole and systole correlated positively with age (ρ=0.6359, ρ=0.7203, ρ=0.5937, and ρ=0.6690, respectively; *P*=0.003, *P*<0.001, *P*=0.007, and *P*=0.0017, respectively). E/Em at the LV lateral and septal walls (ρ=0.7062 and ρ=0.8384;

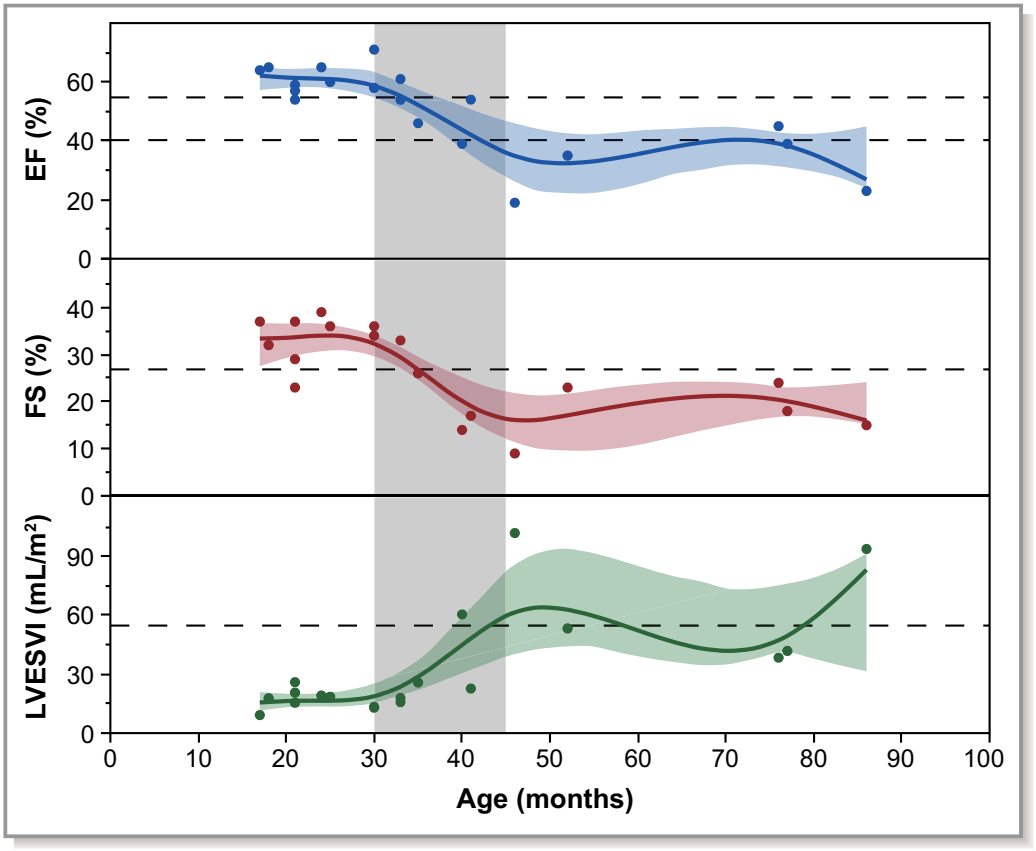

Figure 2. Regressions of age vs EF, FS, and LVESVI in echocardiography shown by fit splines. Data from 19 golden retriever muscular dystrophy dogs in the single-time-point echocardiographic study demonstrate correlations between age and EF, FS, and LVESVI. Age correlated negatively with EF and FS ($\rho=-0.7866$ and $\rho=-0.6991$; $P<0.001$ for both), and positively with LVESVI ($\rho=0.7203$; $P<0.001$). The smoothing fit splines ($\lambda=0.05$; $R^2>75\%$) were obtained to best fit the data points and predict the values at different ages. The splines showed a more dramatic change around the 30 to 45 month period (gray color area). The blue, red, and green color regions represent the confidence of fit. Phenotypic variation and low numbers of older dogs influenced the accuracy of splines later in the disease course. The black dash lines represent the clinical cut off values of systolic dysfunction (EF of 55% in DMD; EF of 40%, FS of 27%, and LVESVI of 55 mL/m^2 in canine dilated cardiomyopathy). Based on the fit splines, EF fell to 53.78% at age 34 months and to 38.82% at age 43 months. FS fell to 26.82% at 35 months. LVESVI increased to 57.29 mL/m^2 at 44 months. Taken together, our results indicate that systolic dysfunction occurs between 30 to 45 months of age. EF indicates ejection fraction; FS, fractional shortening; LVESVI, left ventricular end-systolic volume index.

$P<0.001$ for both) and isovolumic relaxation time ($\rho=0.6530$; $P=0.03$) all positively correlated with age, whereas LV lateral wall peak early diastolic myocardial velocity and ratio of peak early/late diastolic myocardial velocity in tissue Doppler imaging correlated negatively ($\rho=-0.4653$ and $\rho=-0.5529$, respectively; $P=0.04$ for both).

Timeline of Systolic Dysfunction

To understand the timeline of systolic dysfunction, we used data from EF, FS, and LVESVI to obtain age correlation fit splines (Figure 2). Smoothing fit splines, with $\lambda=0.05$ and $R^2>75\%$, were obtained to best fit the data points and the trending of each variable. The splines were also used to predict the values at different ages. A more dramatic change of splines was found around the 30- to 45-month period for EF, FS, and LVESVI. Phenotypic variation and the number of older dogs influenced the accuracy of splines at older ages. We used spline fitting because it allows sections of data to be represented in a piecewise fashion (spline curve) compared with linear regression, which considers the data set as a whole.[32,33] In comparing the 2 approaches (not shown), spline better fit the data points, especially at the age of <45 months, allowing us to more accurately predict the onset of systolic dysfunction. Importantly, spline could potentially overfit segments of the line derived from few data points, so the

disease course predicted for older dogs must be interpreted cautiously.

Both the generally accepted standard of EF <55% in DMD patients[34–36] and EF <40% in canine dilated cardiomyopathy[37] were assessed, with EF falling to 53.78% at 34 months of age and 38.82% at 43 months. The value for FS fell to 26.82%, below the generally accepted level of <27% used to define systolic dysfunction in humans and dogs,[36,38] at 35 months. LVESVI increased to 57.29 mL/m^2, beyond the value of >55 mL/m^2 used to define systolic dysfunction in canine dilated cardiomyopathy,[28] at 44 months of age. Fitting these collective results to our age groups, systolic dysfunction occurred between 30 to 45 months of age.

Longitudinal Comparison of Circumferential Strain and Strain Rate Versus EF

In our longitudinal study, average circumferential strain and EF showed a trend (P=0.06 for both) toward worsening over the 12-month period in the 10 GRMD dogs. We further separated the 10 dogs into 2 groups based on the age of the first echocardiography examination, either 10 months (n=4) or 22 months (n=6; Figure 3). Circumferential strain did not differ over the 12-month period in dogs imaged initially at 10 months but did worsen (values became less negative) significantly in the 22-month group (P=0.03). In contrast, neither EF nor circumferential strain rate differed in either age group over the 12-month period (P>0.05 for all). Taken together, these data suggest that circumferential strain is more sensitive than EF and circumferential strain rate in early disease detection.

We further compared the segmental circumferential strain and strain rate in the 2 age groups (Table S3). In the 10-month group, neither circumferential strain nor strain rate differed over the 12-month period for any of the segments (P>0.05 for all). In the 22-month group, although circumferential strain of the anteroseptal and inferior segments worsened (P=0.03 for both), the circumferential strain rate did not differ for any of the segments (P>0.05 for all).

Comparison of LV Function in CMR Between Age Groups

As in the single-time-point echocardiographic study, the dogs were divided into 3 age groups for CMR LV functional analysis (Table S4): <30 months (n=8), 30 to 45 months (n=4), and >45 months (n=2). Values of LVEDV, LVESV, and myocardial mass were higher at >45 versus <30 months (P=0.04, P=0.049, and P=0.03, respectively). Body weight, BSA, EF, and BSA-indexed values of LVEDV (LVEDVI) and myocardial mass at end-diastole differed among the age groups with the Kruskal–Wallis test (P=0.02, P=0.02, P=0.045, P=0.045, and P=0.03, respectively) but not with the Dunn test (P>0.05). Values for BSA-indexed LVESV (LVESVI) did not differ (P>0.05) among the age groups. The lower EF values in CMR were likely due to the suppressive effect of general anesthesia.[39,40]

Correlations Between CMR Variables and Age

Correlations between CMR variables and age are listed in Table 1. We found EF correlated negatively with age (ρ=−0.7766; P=0.0011), consistent with declining cardiac function. LVEDVI, LVESVI, and index of myocardial mass at end-diastole all positively correlated with age (ρ=0.7567, ρ=0.7146, and ρ=0.7412, respectively; P=0.0017, P=0.004, and P=0.002, respectively), in keeping with progressive dilated cardiomyopathy.

Myocardial Lesions and LGE

In this study, we analyzed LGE scores from the dogs by using 2 different approaches.

Approach 1: LGE-heart

We calculated the mean LGE score (LGE-heart) from 16 myocardial segments of each dog:

$$\text{LGE-heart} = (\text{LGE score of segment } 1 + 2 + 3\ldots + 16)/16$$

The LGE-heart value represented the mean LGE score of each dog's heart. LGE-heart was further correlated with the age of the 15 dogs imaged with LGE. LGE-heart positively correlated with age (ρ=0.7794; P<0.001). We also correlated LGE-heart with EF from the 12 dogs that had sufficient imaging quality for EF measurements. LGE-heart negatively correlated with EF (ρ=−0.8225; P=0.0010). Taken together, LGE heart, age, and EF were all correlated (Figure 4A).

Approach 2: LGE-segment

To determine the distribution of myocardial lesions across different LV segments, we divided the 15 dogs into the same 3 age groups: <30 months (n=7), 30–45 months (n=5), and >45 months (n=3). We further calculated the mean LGE score for each myocardial segment (LGE-segment; 1–16). For instance, in the <30-month group, the equation for segment 1 was:

$$\text{LGE-seg1} = (\text{LGE score of segment 1 in dog } 1 + 2 + 3\ldots + 7)/7$$

LGE-segment for the 16 myocardial segments was calculated for each age group, and these results were transformed into grayscale images (Figure 4B). Using this method, the LV

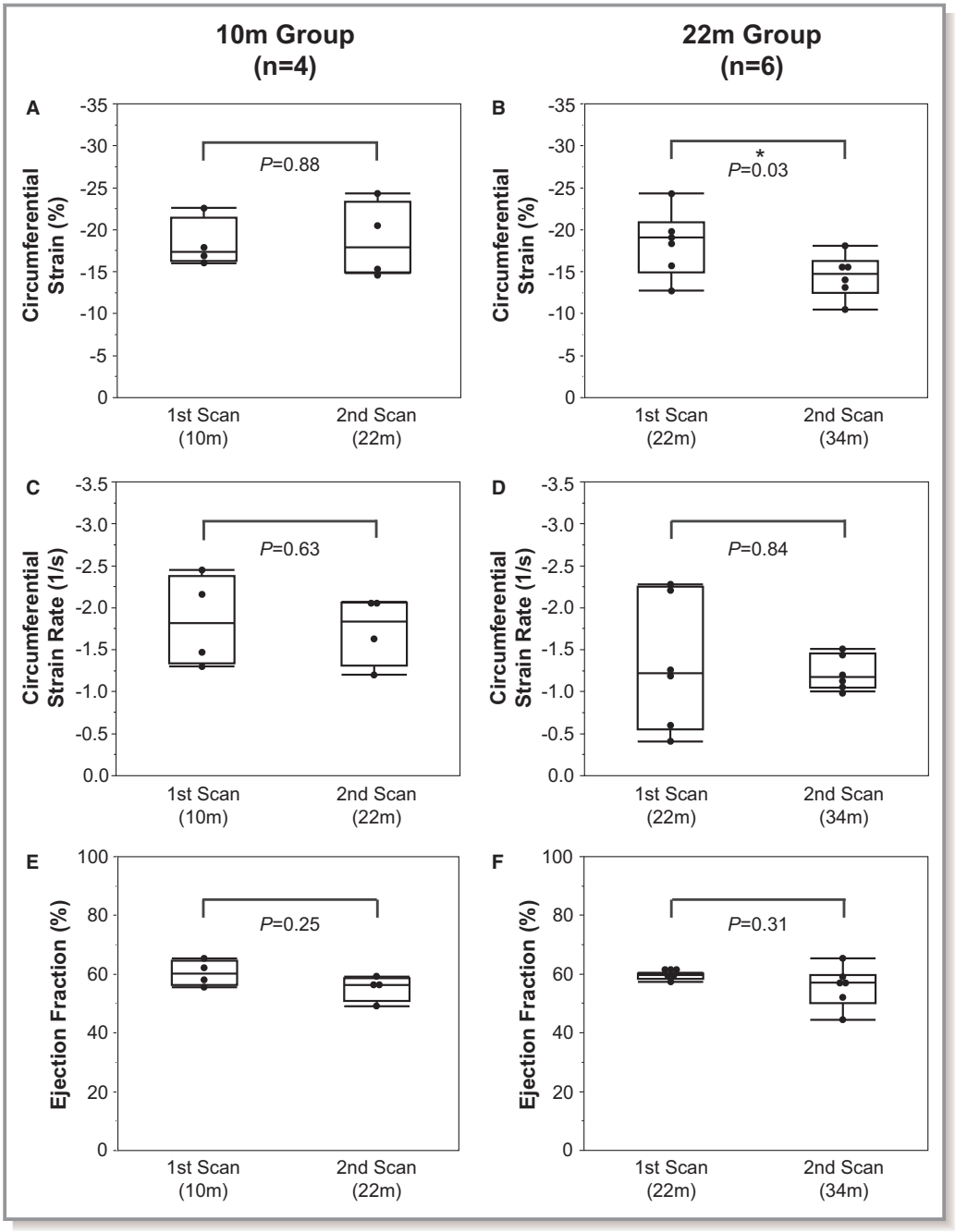

Figure 3. Changes of average circumferential strain, strain rate, and EF in the longitudinal study. The 10 dogs in the study were separated into 2 groups based on age at the first echocardiographic examination, either 10 months (n=4) or 22 months (n=6). In the 10-month group, no difference was found in circumferential strain (P=0.88) (**A**), circumferential strain rate (P=0.63) (**C**), and EF (P=0.25) (**E**) over the 12-month period. In the 22-month group, circumferential strain showed a significant change (P=0.03) at 34 months (**B**), whereas neither EF (P=0.31) (**F**) nor circumferential strain rate (P=0.84) (**D**) differed over the 12-month period, suggesting that circumferential strain is more sensitive than EF and strain rate in early disease detection at the age of 22 to 34 months. *P<0.05. EF indicates ejection fraction.

anteroseptal and lateral to inferior regions had greater enhancement, consistent with more marked fibrosis. The basal and mid-LV anteroseptal segments (segments 2 and 8) also showed early enhancement at <30 and 30 to 45 months. Overall, the distribution and severity of LGE lesions gradually increased over time in all myocardial segments.

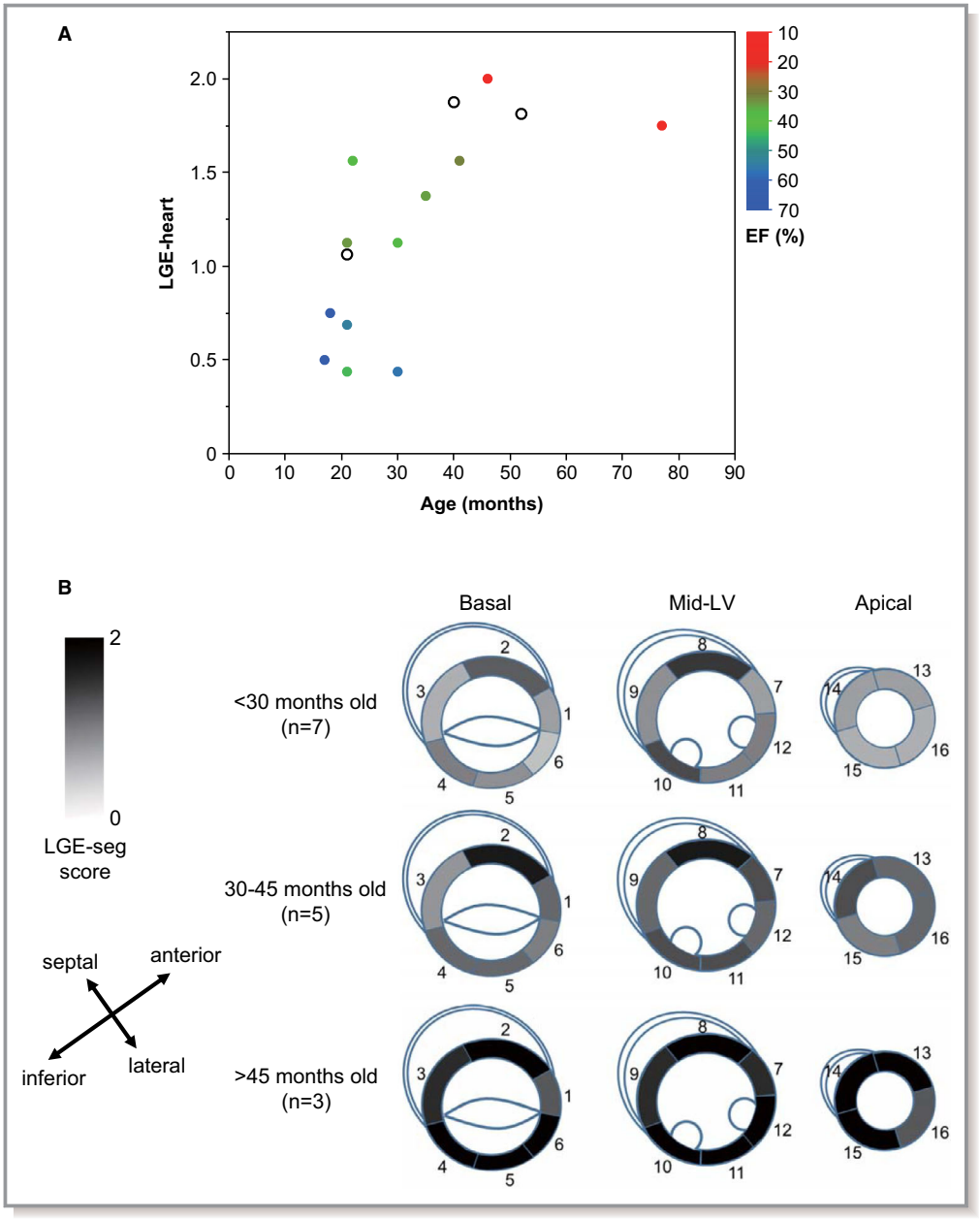

Figure 4. LGE during disease progression. **A**, Correlations between LGE-heart, age, and EF. LGE-heart represents the mean LGE score of each dog's heart (n=15). Data point colors reflect EF values of different golden retriever muscular dystrophy dogs (n=12). Three dogs that did not have sufficient image quality for EF measurements are shown as unfilled circles. LGE-heart correlated positively with age (ρ=0.7794; P<0.001) and negatively with EF (ρ=−0.8225; P=0.0010). Taken together, LGE-heart, age, and EF were all correlated. Older dogs showed higher LGE-heart scores, in accordance with lower EF values. **B**, LGE progression among myocardial segments. LGE-segment for 3 age groups are shown in grayscale to indicate the severity of LGE lesions. Darker shades indicate greater LGE, likely reflecting a more severe myocardial lesion. The degree of LGE became more severe and diffuse with age, as disease progressed. The left ventricle (LV) anteroseptal and lateral to inferior regions showed greater enhancement, likely reflecting regions more affected by the fibrosis. EF indicates ejection fraction; LGE, late gadolinium enhancement.

Pathological assessment

Eight dogs were humanely euthanized within 7 days of the imaging assessment and necropsies were performed. These pathological findings are part of a separate comprehensive natural history study of GRMD cardiac pathology (unpublished data: S.M. Schneider, DVM, PhD and J.N. Kornegay, DVM,

PhD, 2019). Based on our pathological findings, the extent of fibro-fatty myocardial lesions generally corresponded with the imaging results (Figure 5).

Scoring System for GRMD Cardiomyopathy: Cardiac Score and Cardiomyopathy Score

Using echocardiography and CMR median values at 30 to 45 and >45 months (Tables S2 and S4), we established a multiparametric scoring system to assess the severity of cardiomyopathy (Table 2). A score of 0, 1, or 2, representing normal to increasing disease severity, was assigned for each parameter in the 3 categories of systolic function, diastolic function, and LV chamber enlargement. The systolic-function score was based on the average score of EF, FS, and circumferential strain from echocardiography and EF from CMR. The diastolic function score was obtained using the average score of E/Em (LV lateral) and E/Em (LV septal). The LV enlargement score was based on the average score of LVEDVI, LVESVI, and normalized LV internal diameters in diastole and systole from echocardiography and LVEDVI and LVESVI from CMR. The sum of the systolic function score, the diastolic function score, and the LV enlargement score designated the cardiac score (range: 0–6), with higher values indicating more severe functional and morphological changes.

Cardiac scores were calculated for all 19 dogs (aged 17–86 months; 14 male, 5 female) in our single-time-point echocardiographic study. Nine of these 19 dogs (aged 17–77 months; 6 male, 3 female) had CMR LV functional data and 12 (aged 17–77 months; 8 male, 4 female) had CMR LGE data within 1 day of echocardiography. Using the Spearman correlation coefficient, we found that cardiac score correlated positively with age (n=19; ρ=0.8323; P<0.001). Furthermore, the results of LGE-heart highly and positively correlated with cardiac score (n=12; ρ=0.9437; P<0.001; Figure 6A). Accordingly, a further score of 0 to 2 for LGE-heart in CMR, reflecting the severity of myocardial fibrosis, was added to give an overall cardiomyopathy score of 0 to 8 in the 12 dogs with LGE-heart results. Cardiomyopathy score correlated positively with age (n=12; ρ=0.8290; P<0.001) and generally tracked with cardiac scores to represent both functional and fibrotic severity of cardiomyopathy in individual dogs (Figure 6B). As with data to determine the timeline for systolic dysfunction, smoothing fit splines (λ=0.05 and R^2>80%) were used. Considering the scoring system in the context of the timeline for systolic dysfunction, at the ages of 30 to 45 months, the

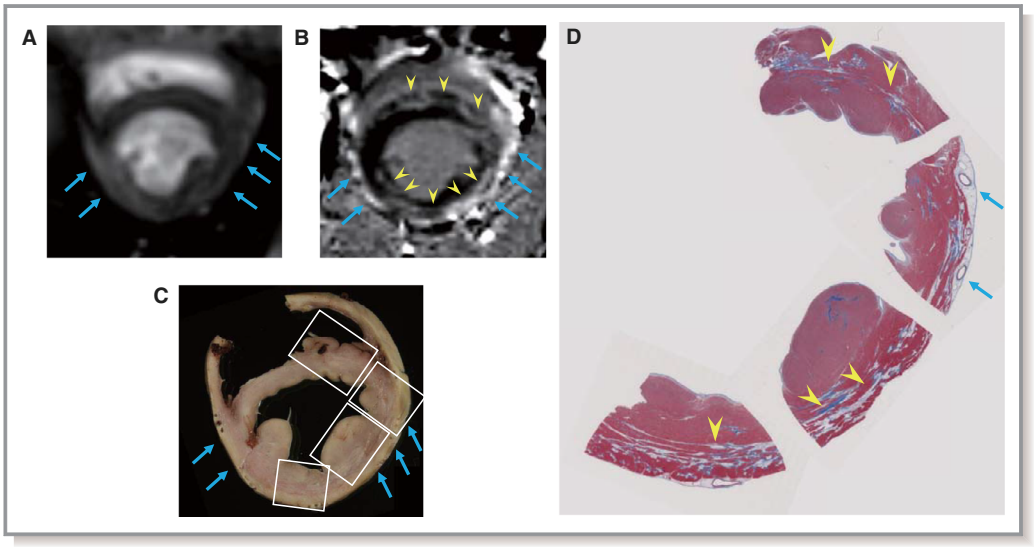

Figure 5. Precontrast (**A**) and postcontrast (**B**) cardiac magnetic resonance images and gross (**C**) and histopathologic (**D**) sections from a 41-month-old male golden retriever muscular dystrophy dog. Areas of increased signal intensity, most likely representing combined pericardial and epicardial fat (blue arrows) were clearly seen in the postcontrast phase-sensitive inversion recovery LGE image (**B**) and, to a lesser extent, in the precontrast FLASH image (**A**). Additional intramyocardial areas of increased signal intensity, reflecting LGE, could also be seen in the left ventricle (LV) inferior to lateral wall and anterior septum in panel B (yellow arrowheads). Corresponding areas of myocardial fatty deposition were not as obvious in the precontrast FLASH image in **A** and would be indistinguishable from fibrosis in **B**. The pathological sections in **C** (formalin-fixed slice) and **D** (trichrome stain) were approximately at the same level as the images in **A** and **B**. Areas of peripheral pallor in **C** (blue arrows) and vacuolation in **D** (yellow arrowheads) correspond to the increased signal intensity seen in **A** and **B**. FLASH indicates fast low-angle shot; LGE, late gadolinium enhancement.

Table 2. Criteria of Cardiac Scoring System

	Score 0	Score 1	Score 2
Systolic function			
EF, %	>54	54 to >35	≤35
FS, %	>33	33 to >18	≤18
Circumferential strain, %	<−24.24	−24.24 to <−10.12	≥−10.12
EF from CMR, %	>35.95	35.95 to >12.35	≤12.35
Systolic function score (0–2) = (Total score of EF and/or FS and/or Circ Strain and/or EF from CMR) / number of included markers			
Diastolic function			
E/Em (LV lateral)	<6.50	6.50 to <9.38	≥9.38
E/Em (LV septal)	<9.495	9.495 to <11.25	≥11.25
Diastolic function score (0–2) = (Total score of LV lateral E/Em and/or LV septal E/Em) / number of included markers			
LV enlargement*			
LVEDVI, mL/m^2	<44.71	44.71 to <84.25	≥84.25
LVESVI, mL/m^2	<17.90	17.90 to <53.30	≥53.30
LVIDd-n, cm/kg	<1.54	1.54 to <1.94	≥1.94
LVIDs-n, cm/kg	<1.02	1.02 to <1.40	≥1.40
LVEDVI from CMR, mL/m^2	<66.21	66.21 to <130.28	≥130.28
LVESVI from CMR, mL/m^2	<39.08	39.08 to <114.80	≥114.80
LV enlargement score (0–2) = (Total score of LVEDVI and/or LVESVI and/or LVIDd-n and/or LVIDs-n and/or LVEDVI from CMR and/or LVESVI from CMR) / number of included markers			
Cardiac score (0–6) = Systolic function score (0–2) + Diastolic function score (0–2) + LV enlargement score (0–2) **Cardiomyopathy score (0–8) = Cardiac score (0–6) + LGE-heart (0–2)**			

BSA indicates body surface area; CMR, cardiac magnetic resonance; E/Em, ratio of the mitral valve E wave to early diastolic myocardial velocity in tissue Doppler imaging; EF, ejection fraction; FS, fractional shortening; LGE-heart, late gadolinium enhancement score of the heart; LV, left ventricular; LVEDV, left ventricular end-diastolic volume; LVESV, left ventricular end-systolic volume; LVEDVI, left ventricular end-diastolic volume index; LVESVI, left ventricular end-systolic volume index; LVIDd-n, normalized left ventricular internal diameter in diastole; LVIDs-n, normalized left ventricular internal diameter in systole.
*LVEDVI and LVESVI are the indexed values after BSA normalization (LVEDV/BSA; LVESV/BSA). LVIDd-n and LVIDs-n are the values after body mass normalization using a specific method (Data S1).

cardiac and cardiomyopathy scores were 1.39 to 4.65 and 2.19 to 6.61, respectively.

Correlations Between Cardiac and Skeletal Muscle Functions in GRMD

To understand the relationship between cardiac function and skeletal muscle disease in GRMD, we compared our cardiac results with skeletal muscle measurements in dogs that had both tests within a period of 45 days. The skeletal muscle measurement was performed using established protocols[10,41] in unrelated studies. Skeletal muscle tests included body mass normalized tibiotarsal joint isometric tetanic extension and flexion torque and percentage of eccentric contraction

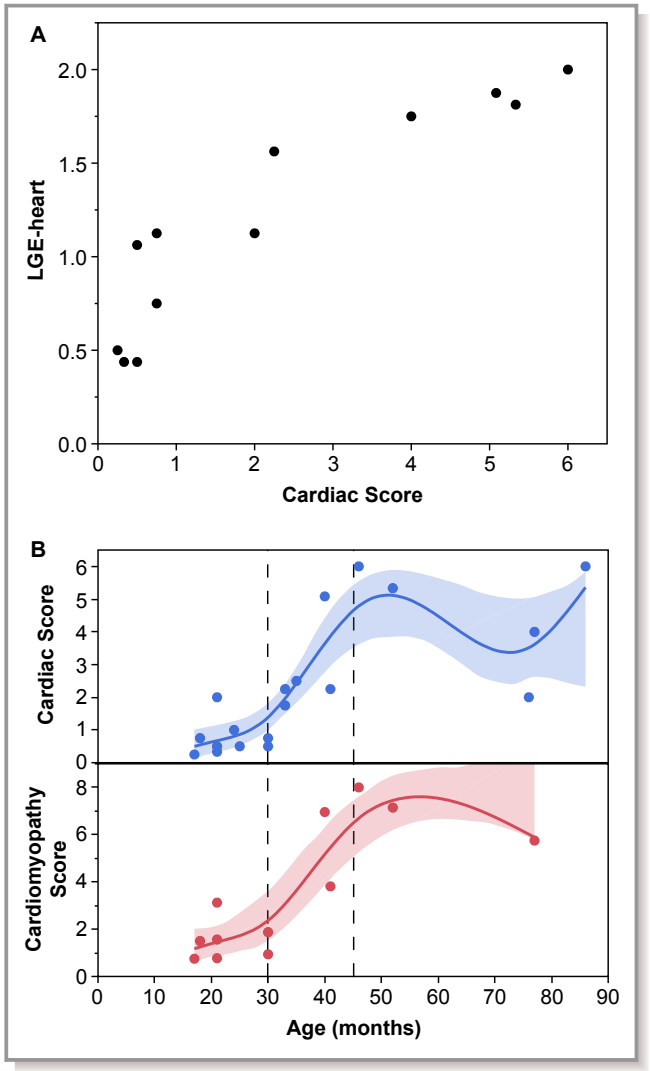

Figure 6. Progression of cardiac scores (n=19) and cardiomyopathy scores (n=12). **A**, Cardiac score correlated positively with LGE-heart (n=12; ρ=0.9437; P<0.001). **B**, Cardiac and cardiomyopathy scores, shown by fit splines, both correlated positively with age (n=19 and n=12, respectively; ρ=0.8323 and ρ=0.8290, respectively; P<0.001 for both) and generally tracked together with increasing severity of cardiac disease in individual dogs. The fit splines (λ=0.05; R^2>80%) represent overall disease progression. Cardiac and cardiomyopathy scores were 1.39 to 4.65 and 2.19 to 6.61, respectively, at the age of 30 to 45 months (vertical black dashed lines). The blue and red regions represent the confidence of fit. Phenotypic variation and low numbers of older dogs influenced the accuracy of splines and widened the confidence of fit later in the disease course. LGE-heart indicates the late gadolinium enhancement score of the heart.

decrement after 10 and 30 stretches. Overall, data from 11 dogs (aged 17–77 months; 9 male, 2 female) with both echocardiography and skeletal muscle measurements and 10 dogs (aged 9–77 months; 5 male, 5 female) with CMR and skeletal muscle measurements were analyzed using the Spearman correlation coefficient (Table 3). Normalized tetanic flexion torque negatively correlated with age (ρ=−0.7982; *P*=0.003; Figure 7) and cardiac score (ρ=−0.8246; *P*=0.002). Normalized tetanic flexion torque positively correlated with EF and FS from echocardiography (ρ=0.7123 and ρ=0.8128; *P*=0.014 and *P*=0.002) and EF from CMR (ρ=0.6848; *P*=0.03), in keeping with concurrent progressive skeletal muscle and cardiac disease. None of the values for normalized tetanic extension torque or eccentric contraction decrement after 10 or 30 stretches correlated with age or cardiac variables.

Table 3. Correlation Among Skeletal Muscle Measurements, Age, and Cardiac Function Variables

Variable*	Spearman ρ	*P* Value
Body mass normalization		
Normalized tetanic flexion torque, Nm/kg		
Age, mo	−0.7982	0.003§
EF, %	0.7123	0.014‡
FS, %	0.8128	0.002§
EF from CMR, %†	0.6848	0.03‡
Cardiac score	−0.8246	0.002§
Normalized tetanic extension torque, Nm/kg		
Age, mo	0.0459	0.89
EF, %	−0.4932	0.12
FS, %	−0.1416	0.68
EF from CMR, %†	0.0909	0.80
Cardiac score	0.1367	0.69
Eccentric contraction decrement		
ECD1–10, %		
Age, mo	0.3486	0.29
EF, %	−0.1142	0.74
FS, %	−0.0320	0.93
EF from CMR, %†	0.4061	0.24
Cardiac score	0.2916	0.38
ECD1–30, %		
Age, mo	0.1193	0.73
EF, %	0.1142	0.74
FS, %	−0.0228	0.95
EF from CMR, %†	0.1394	0.70
Cardiac score	−0.0228	0.95

CMR indicates cardiac magnetic resonance; ECD1–10, eccentric contraction decrement after 10 stretches; ECD1–30, eccentric contraction decrement after 30 stretches; EF, ejection fraction; FS, fractional shortening.
*Eleven dogs in a single-time-point echocardiographic study were included for analysis.
†Ten dogs in a CMR study were included for analysis.
‡*P*<0.05.
§*P*<0.01.

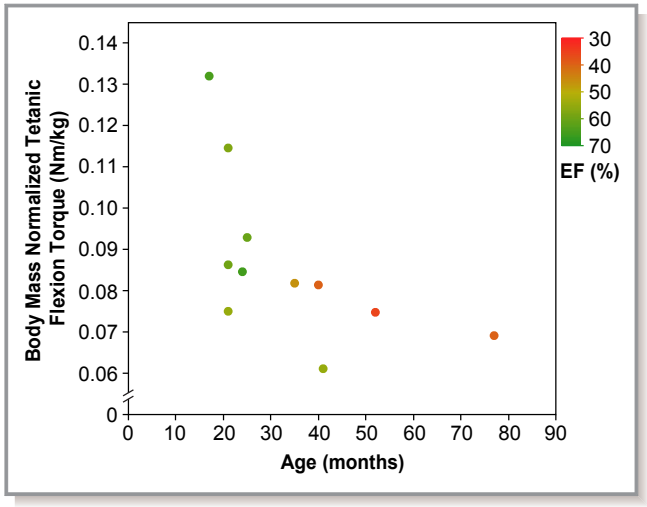

Figure 7. Correlations between body mass normalized tibiotarsal joint tetanic flexion torque, age, and EF from echocardiography (n=11). Data point colors reflect EF values of GRMD dogs. Normalized tetanic flexion torque negatively correlated with age (ρ=−0.7982; *P*=0.003) and positively correlated with EF (ρ=0.7123; *P*=0.014). Older GRMD dogs had lower tetanic flexion torque and EF values. EF indicates ejection fraction; GRMD, golden retriever muscular dystrophy.

Discussion

With improved respiratory care, cardiomyopathy now accounts for the majority of DMD deaths.[42] Studies in animal models are needed to better define the pathogenesis of cardiac involvement and evaluate treatment regimens. GRMD dogs generally have a more severe cardiac phenotype[18,19,22–24] compared with *mdx* mice, in keeping with the progressive disease seen in DMD.[43,44] However, limited natural history studies are available in GRMD dogs, particularly beyond 1 year of age. In our current study, we defined the clinical course of GRMD cardiomyopathy by assessing echocardiography and CMR imaging in adult dystrophic dogs. Our study showed GRMD dogs have progressive cardiomyopathy characterized by LV systolic and diastolic dysfunction, LV chamber enlargement, myocardial strain abnormalities, and myocardial fibrosis similar to that seen in DMD.

Because of X-linked inheritance, most DMD patients are boys and men. For the sake of the GRMD model, affected males are bred to carrier females, producing 25% each normal males, carrier females, and both dystrophic hemizygous males and homozygous females. A previous study from our

laboratory did not show differences in skeletal muscle function between hemizygous male and homozygous female dogs.[26] Similarly, in an as yet unpublished study (L.-J. Guo, DVM, MS and J.N. Kornegay, DVM, PhD, 2019) of younger GRMD dogs from our laboratory, cardiac function did not differ between males and females. For the current study of adult dogs, fewer females were available for study; for instance, only 2 females versus 8 males were included in the longitudinal echocardiographic study. Our ability to distinguish a sex effect was further compounded by the fact that males and females were not age matched. Consequently, results from both sexes were analyzed together in this study.

We previously managed a number of adult GRMD dogs with clinical cardiac disease.[10] Data from these and other affected dogs could potentially be used to compare the efficacy of different treatment regimens. Such studies would be facilitated if the approximate age at which systolic dysfunction occurred in GRMD were known. Using echocardiography, EF, FS, and circumferential strain were all sensitive for predicting the decline of LV function during disease progression. Furthermore, using multiple clinical standards of systolic dysfunction that are typically assessed in DMD and canine dilated cardiomyopathy, we found that systolic dysfunction in GRMD dogs tended to develop between 30 to 45 months of age. This period offers a window in which treatments could be tested in GRMD dogs in our breeding colony, just as we have used the age period of 3 to 6 months to assess therapies directed toward skeletal muscle.[10] However, practical, largely financial, restraints exist in maintaining dogs until this age. For this reason, markers that can differentiate dystrophic and normal dogs at earlier ages are needed to facilitate preclinical testing. Preclinical studies would also be facilitated by standardizing categories of disease severity, as with the cardiac scoring system discussed later, instead of relying on the dog's absolute age.

Notably, several GRMD dogs in the >45-month group had signs of compromised systolic function, consistent with congestive heart failure in the late stages of cardiomyopathy. Not surprisingly, the cardiac phenotype of some affected dogs deviated from this pattern, consistent with variable heart disease seen in both DMD and GRMD. The progressive decline of systolic function over the 30- to 45-month period, with an associated wider range of results, likely precluded reaching statistical significance when we compared EF and FS between the 2 younger age groups (<30 versus 30 to 45 months). However, in our longitudinal study, circumferential strain appeared more sensitive than EF in identifying systolic dysfunction in GRMD, potentially allowing detection of disease as early as 22 to 34 months of age. These results parallel those from DMD boys,[34,36,45–48] who show early changes in circumferential strain followed by progressive systolic dysfunction. Myocardial strain measures are also known to precede systolic dysfunction in other inherited diseases, including hypertrophic cardiomyopathy,[49] LV noncompaction,[50] acquired cardiomyopathies secondary to myocarditis,[51] and chemotherapy exposure.[52] Furthermore, several studies have demonstrated a correlation between decreased strain measures and the presence of LGE in heart disease.[53–55] Extending this work to segmental analysis, studies have shown that circumferential strain in young DMD patients differs from normal in the anteroseptal, inferior, and inferolateral segments.[45] Our segmental strain analysis showed analogous early changes in circumferential strain of the LV anteroseptal and inferior wall. Taking these results together, this study not only identified the timing of systolic dysfunction in GRMD dogs but also validated multiple imaging markers to assess systolic function in the progression of GRMD cardiomyopathy.

We also identified a progressive decline in diastolic function with echocardiography, similar to that of DMD.[36,56] Most importantly, E/Em at the LV septal and lateral wall correlated positively with age, suggesting that this ratio could be a sensitive marker of diastolic dysfunction. A comparison among values from the 3 age groups also showed that MV A velocity was increased at >45 months, with an associated decrease in E/A ratio. Similar results are seen in DMD patients,[36] consistent with an increase of left atrial contraction to compensate for ventricular diastolic dysfunction. Although diastolic dysfunction is thought to predate systolic involvement in DMD,[56] the limited number of dogs in our study precluded reaching a similar conclusion. Overall, our data suggest that application of Doppler flow and tissue Doppler imaging to track the E/Em provides a sensitive marker to longitudinally assess progression of diastolic dysfunction in GRMD.

In DMD and GRMD, availability of instrumentation and technical issues are important in cardiac assessment. Speckle tracking technology required to measure circumferential strain is usually included in advanced ultrasound machines. As an added advantage, circumferential strain provides direct measurement of myocardial motion, which is more sensitive for the subclinical phase in DMD.[36] In contrast, postural changes in both dystrophic boys and dogs limit the acoustic window achieved with echocardiography. Ideally, EF, FS, and circumferential strain should all be measured during the scan, but these measurements may be difficult because of poor imaging quality in echocardiography. Postural restrictions are not a limitation with CMR,[57] making it an attractive alternative.[34,58] In our study, EF from echocardiography and CMR both correlated well with age, suggesting that either technique is sufficiently sensitive to demonstrate disease progression. However, the necessity for anesthesia with CMR in dogs depresses EF, which complicated evaluation of systolic dysfunction in our study. The fact that CMR results have not

been established in normal golden retrievers further limited interpretation. Accordingly, CMR will undoubtedly become an even more valuable technique for GRMD dogs when additional reference data are established.

GRMD dogs had progressive increases in BSA-indexed LV chamber sizes on both echocardiography and CMR, consistent with dilated cardiomyopathy of DMD. Progressive ventricular dilation presumably occurs because of ongoing cardiac muscle degeneration, with associated congestion of the heart. Several GRMD dogs with cardiac chamber dilation also showed valvular regurgitation, mostly involving the mitral valve. This regurgitation further compromised congestive heart failure over the disease course. Despite these changes, LV wall thickness did not decrease until very late in the disease. As a result, the myocardial mass progressively increased during the disease process, in line with pathological eccentric hypertrophy.[59] Importantly, in addition to changes in myocardial mass, fibrosis also affects cardiac function in this cardiomyopathy.

LGE is commonly used to identify myocardial fibrosis in DMD patients and tracks with cardiac functional parameters such as decreased EF.[60] In principle, gadolinium persists in the extracellular matrix of fibrotic lesions longer than in normal tissue, causing persistent contrast enhancement in the CMR LGE images.[61] As with DMD,[60] the severity of LGE correlated with EF in GRMD dogs in this study. In DMD patients, LGE is first seen in the basal area at the LV inferolateral wall.[62] Our GRMD LGE images showed analogous myocardial contrast enhancement. The lesions of GRMD commonly occurred in the inferior, inferolateral, and anteroseptal walls from the basal to mid-LV levels. These lesions corresponded with hyperechoic regions seen in the LV free wall on echocardiography, as originally reported by Moise et al.[18] Early evidence of LGE septal involvement in these dogs contrasts with the late onset of septal changes in DMD.[60] However, as discussed earlier, strain analysis in both DMD and GRMD has shown early septal involvement. In addition, there was more diffuse LGE in the hearts of older dogs, potentially representing the combined effects of cardiac fibrosis and fatty deposition.[63]

Notably, the nature of LGE changes differed among dogs in this study, in keeping with the variable nature of lesions in DMD patients. We were unable to fully characterize these lesions because of suboptimal image quality. Although we attempted to focus our LGE studies on the myocardium, enhancement caused by epicardial fat may have obscured some lesions. The limited number of dogs between 6 and 30 months of age restricted our ability to determine whether LGE changes predated systolic dysfunction. Further comparisons between LGE patterns and pathological results would be necessary to better characterize the distribution of fibrotic and fatty lesions among GRMD dogs. The most comprehensive, yet limited, pathological study of the GRMD cardiomyopathy showed that all dogs aged $\geq$1 year had fibrosis in the subepicardial region of the LV free wall, the LV papillary muscles, and the right ventricular aspect of the septum.[19] Our results were generally consistent with these findings. Nonetheless, the suboptimal nature of the LGE images precluded us from definitively confirming that fibrosis began in the subepicardial area. The pathological results shown in Figure 5 demonstrated fibro-fatty infiltration in the dystrophic hearts in regions corresponding to our LGE findings.

Given unavailability of instrumentation and technical challenges, some echocardiographic and CMR imaging markers reported in this study may not be assessed by other research groups. To compensate for any missing tests, we developed a multiparametric approach to establish a "cardiac score" that considered several indexes for systolic and diastolic functions and LV chamber size. LGE results were also included, when available, to provide a "cardiomyopathy score" and additional insight on the degree of myocardial fibrosis. Because GRMD cardiomyopathy progresses at a variable rate, these scores give an index of overall disease progression and have the potential to differentiate dogs between different phenotypes.

The relationship between skeletal muscle and cardiac disease remains unclear in DMD. An early study by Heymsfield et al suggested that skeletal and cardiac muscle disease progressed at different rates.[64] Conversely, Posner et al showed that FS correlated with quantitative muscle testing among nonambulatory DMD patients,[65] indicating that skeletal and cardiac function were directly related. Studies from *mdx* mice have been inconclusive, with rescue of skeletal muscle having positive, negative, or no effects on cardiac function.[66–68] In agreement with the findings of Posner et al in DMD, multiple cardiac imaging markers from our GRMD dogs, including EF, FS, and cardiac score, correlated with normalized tibiotarsal tetanic flexion torque. Dogs with more severe cardiac dysfunction had lower flexion torque values, suggesting—for the first time—a direct relationship between the decline in cardiac and skeletal muscle function in the GRMD model. Importantly, although we have not systematically assessed skeletal muscle function in adult GRMD dogs, previous studies of younger dogs have shown differential loss of extensor and flexor muscle strength over time.[41] Therefore, it is not surprising that the cardiac indexes assessed in this study did not correlate with other skeletal muscle function tests.

GRMD colonies worldwide were derived from a golden retriever dog originally studied by our group.[43] All of these colonies have been outbred, such that GRMD is no longer a disease of purebred GRMD dogs. Potentially because of differences in genetic background, the phenotypes of dystrophic dogs in GRMD colonies vary, with some tending to have a more severe phenotype than dogs in our original

colony. For instance, dogs from the colony at Alfort in France often lose the ability to walk by 6 months,[69] and many from the Brazilian colony at the University of São Paulo die before 2 years of age.[70] Because of the rapidity of skeletal muscle progression in these dogs, the cardiomyopathy may not fully develop before euthanasia is required. Alternatively, use of more sensitive cardiac markers, as with myocardial velocity gradient in the French colony, could allow detection of preclinical disease.[22,71,72] Unfortunately, relatively few dogs from our study had the specific imaging recording for gradient analysis. Importantly, with genetic[73,74] and cell-based therapies,[75] the lives of GRMD dogs could be extended, allowing for further progression of the cardiac changes. Therefore, understanding the overall natural history of this cardiomyopathy is essential for future therapeutic testing. With this increasing need, development of the multiparametric cardiac and cardiomyopathy scores should increase the likelihood that results from GRMD studies can be extrapolated among the different colonies worldwide. These scores also provide a standardized method to categorize the severity of the GRMD cardiomyopathy without strict consideration of age. Based on our results, cardiac and cardiomyopathy scores of 1.39 to 4.65 and 2.19 to 6.61, respectively, would be the appropriate stage of disease for preclinical cardiac testing. The image quality, availability of CMR and LGE, and study focus would dictate which score would be appropriate for the study.

Although this study substantially advanced our understanding of the natural history of GRMD cardiomyopathy, several limitations exist. By design, only adult dogs were assessed, precluding characterization of the early disease course. Although the study included more dogs and a broader set of imaging modalities than previous studies, the relatively small number of dogs and the phenotypic variation typical of GRMD limited statistical power. The low numbers of dogs also kept us from subdividing dogs into different groups based on cardiac phenotype. In keeping with phenotypic variation, dogs with mild cardiomyopathy could potentially live longer, which would cause overall disease severity to be underestimated. Furthermore, echocardiographic interpretation was compromised in severely affected dogs by their postural changes and irregular cardiac rhythms. Some LGE images collected early in the study were of suboptimal quality because of our need to refine the technique, thus limiting interpretation of myocardial lesions and the semiquantitative analysis.

Conclusions

This study defined the natural history of echocardiographic and CMR findings in adult GRMD dogs with cardiomyopathy. Systolic function was progressively lost, as shown particularly by declining EF and FS and worsening circumferential strain. Thirty to 45 months was the age range at which systolic dysfunction occurred, potentially providing a time when prophylactic therapies could be studied. Circumferential strain was more sensitive than EF in detecting early echocardiographic changes. The regions of LGE in CMR generally corresponded to those of DMD, with evidence of LV lateral wall lesions and even earlier involvement of the anterior septum in GRMD. A multiparametric cardiac scoring system was developed to allow findings to be extrapolated to other GRMD colonies and to provide an index of disease severity without strict consideration of age. Moreover, tibiotarsal joint tetanic flexion torque was progressively lost in tandem with a decline of cardiac function, establishing a relationship between skeletal muscle and cardiac disease. Taken together, this study established remarkable parallels between the progression of cardiomyopathy in dystrophic dogs and boys, further validating GRMD as a model of DMD cardiac disease.

Acknowledgments

We acknowledge Rachel J. Johnson for her technical expertise in collecting the cardiac magnetic resonance data, Dr Sarah M. Schneider for providing the pathological images, and Heather Heath-Barnett for assisting with animal procedures.

Author Contributions

Guo performed the main study and image processing, analyzed data, and wrote the article. Guo and Miller performed the single-time-point echocardiographic scans. Spurney performed the echocardiographic scans and imaging analysis in the longitudinal study. Lenox and Soslow assisted with cardiac magnetic resonance protocol developments. Bettis assisted with animal procedures. Cummings supervised the statistical analysis. Kornegay performed the skeletal muscle measurements. Soslow and Nghiem assisted with the analytic approach and article preparation. Kornegay provided funding for the study. Kornegay and Spurney supervised the overall study and assisted with article preparation. All authors participated in revision of the article.

Sources of Funding

Dogs from this study were from the golden retriever muscular dystrophy breeding colony supported through multiple grants.

Disclosures

Dr Kornegay is a paid consultant for Solid Biosciences. Dr Nghiem is a paid consultant for Agada Biosciences. The remaining authors have no disclosures to report.

References

1. Hoffman EP, Knudson CM, Campbell KP, Kunkel LM. Subcellular fractionation of dystrophin to the triads of skeletal muscle. *Nature*. 1987;330:754–758.
2. Hoffman EP, Brown RH Jr, Kunkel LM. Dystrophin: the protein product of the Duchenne muscular dystrophy locus. *Cell*. 1987;51:919–928.
3. Kamdar F, Garry DJ. Dystrophin-deficient cardiomyopathy. *J Am Coll Cardiol*. 2016;67:2533–2546.
4. Cheeran D, Khan S, Khera R, Bhatt A, Garg S, Grodin JL, Morlend R, Araj FG, Amin AA, Thibodeau JT, Das S, Drazner MH, Mammen PPA. Predictors of death in adults with Duchenne muscular dystrophy-associated cardiomyopathy. *J Am Heart Assoc*. 2017;6:e006340. DOI: 10.1161/JAHA.117.006340.
5. Passamano L, Taglia A, Palladino A, Viggiano E, D'Ambrosio P, Scutifero M, Rosaria Cecio M, Torre V, DE Luca F, Picillo E, Paciello O, Piluso G, Nigro G, Politano L. Improvement of survival in Duchenne muscular dystrophy: retrospective analysis of 835 patients. *Acta Myol*. 2012;31:121–125.
6. Guillaume MD, Phoon CK, Chun AJ, Srichai MB. Delayed enhancement cardiac magnetic resonance imaging in a patient with Duchenne muscular dystrophy. *Tex Heart Inst J*. 2008;35:367–368.
7. Bilchick KC, Salerno M, Plitt D, Dori Y, Crawford TO, Drachman D, Thompson WR. Prevalence and distribution of regional scar in dysfunctional myocardial segments in Duchenne muscular dystrophy. *J Cardiovasc Magn Reson*. 2011;13:20.
8. Buddhe S, Cripe L, Friedland-Little J, Kertesz N, Eghtesady P, Finder J, Hor K, Judge DP, Kinnett K, McNally EM, Raman S, Thompson WR, Wagner KR, Olson AK. Cardiac management of the patient with Duchenne muscular dystrophy. *Pediatrics*. 2018;142:S72–S81.
9. McGreevy JW, Hakim CH, McIntosh MA, Duan D. Animal models of Duchenne muscular dystrophy: from basic mechanisms to gene therapy. *Dis Model Mech*. 2015;8:195–213.
10. Kornegay JN, Bogan JR, Bogan DJ, Childers MK, Li J, Nghiem P, Detwiler DA, Larsen CA, Grange RW, Bhavaraju-Sanka RK, Tou S, Keene BP, Howard JF Jr, Wang J, Fan Z, Schatzberg SJ, Styner MA, Flanigan KM, Xiao X, Hoffman EP. Canine models of Duchenne muscular dystrophy and their use in therapeutic strategies. *Mamm Genome*. 2012;23:85–108.
11. Bulfield G, Siller WG, Wight PA, Moore KJ. X chromosome-linked muscular dystrophy (mdx) in the mouse. *Proc Natl Acad Sci USA*. 1984;81:1189–1192.
12. Cooper BJ, Winand NJ, Stedman H, Valentine BA, Hoffman EP, Kunkel LM, Scott MO, Fischbeck KH, Kornegay JN, Avery RJ, Williams JR, Schmickel RD, Sylvester JE. The homologue of the Duchenne locus is defective in X-linked muscular dystrophy of dogs. *Nature*. 1988;334:154–156.
13. Kornegay JN, Tuler SM, Miller DM, Levesque DC. Muscular dystrophy in a litter of golden retriever dogs. *Muscle Nerve*. 1988;11:1056–1064.
14. Nakamura K, Fujii W, Tsuboi M, Tanihata J, Teramoto N, Takeuchi S, Naito K, Yamanouchi K, Nishihara M. Generation of muscular dystrophy model rats with a CRISPR/Cas system. *Sci Rep*. 2014;4:5635.
15. Larcher T, Lafoux A, Tesson L, Remy S, Thepenier V, Francois V, Le Guiner C, Goubin H, Dutilleul M, Guigand L, Toumaniantz G, De Cian A, Boix C, Renaud JB, Cherel Y, Giovannangeli C, Concordet JP, Anegon I, Huchet C. Characterization of dystrophin deficient rats: a new model for Duchenne muscular dystrophy. *PLoS One*. 2014;9:e110371.
16. Klymiuk N, Blutke A, Graf A, Krause S, Burkhardt K, Wuensch A, Krebs S, Kessler B, Zakhartchenko V, Kurome M, Kemter E, Nagashima H, Schoser B, Herbach N, Blum H, Wanke R, Aartsma-Rus A, Thirion C, Lochmuller H, Walter MC, Wolf E. Dystrophin-deficient pigs provide new insights into the hierarchy of physiological derangements of dystrophic muscle. *Hum Mol Genet*. 2013;22:4368–4382.
17. Quinlan JG, Hahn HS, Wong BL, Lorenz JN, Wenisch AS, Levin LS. Evolution of the mdx mouse cardiomyopathy: physiological and morphological findings. *Neuromuscul Disord*. 2004;14:491–496.
18. Moise NS, Valentine BA, Brown CA, Erb HN, Beck KA, Cooper BJ, Gilmour RF. Duchenne's cardiomyopathy in a canine model: electrocardiographic and echocardiographic studies. *J Am Coll Cardiol*. 1991;17:812–820.
19. Valentine BA, Cummings JF, Cooper BJ. Development of Duchenne-type cardiomyopathy. Morphologic studies in a canine model. *Am J Pathol*. 1989;135:671–678.
20. Spurney CF. Cardiomyopathy of Duchenne muscular dystrophy: current understanding and future directions. *Muscle Nerve*. 2011;44:8–19.
21. Finsterer J, Cripe L. Treatment of dystrophin cardiomyopathies. *Nat Rev Cardiol*. 2014;11:168–179.
22. Chetboul V, Escriou C, Tessier D, Richard V, Pouchelon JL, Thibault H, Lallemand F, Thuillez C, Blot S, Derumeaux G. Tissue Doppler imaging detects early asymptomatic myocardial abnormalities in a dog model of Duchenne's cardiomyopathy. *Eur Heart J*. 2004;25:1934–1939.
23. Fine DM, Shin JH, Yue Y, Volkmann D, Leach SB, Smith BF, McIntosh M, Duan D. Age-matched comparison reveals early electrocardiography and echocardiography changes in dystrophin-deficient dogs. *Neuromuscul Disord*. 2011;21:453–461.
24. Kane AM, DeFrancesco TC, Boyle MC, Malarkey DE, Ritchey JW, Atkins CE, Cullen JM, Kornegay JN, Keene BW. Cardiac structure and function in female carriers of a canine model of Duchenne muscular dystrophy. *Res Vet Sci*. 2013;94:610–617.
25. Bartlett RJ, Winand NJ, Secore SL, Singer JT, Fletcher S, Wilton S, Bogan DJ, Metcalf-Bogan JR, Bartlett WT, Howell JM, Cooper BJ, Kornegay JN. Mutation segregation and rapid carrier detection of X-linked muscular dystrophy in dogs. *Am J Vet Res*. 1996;57:650–654.
26. Kornegay JN, Bogan JR, Bogan DJ, Childers MK, Grange RW. Golden retriever muscular dystrophy (GRMD): developing and maintaining a colony and physiological functional measurements. *Methods Mol Biol*. 2011;709:105–123.
27. Cornell CC, Kittleson MD, Della Torre P, Haggstrom J, Lombard CW, Pedersen HD, Vollmar A, Wey A. Allometric scaling of M-mode cardiac measurements in normal adult dogs. *J Vet Intern Med*. 2004;18:311–321.
28. Wess G, Maurer J, Simak J, Hartmann K. Use of Simpson's method of disc to detect early echocardiographic changes in Doberman Pinschers with dilated cardiomyopathy. *J Vet Intern Med*. 2010;24:1069–1076.
29. Rishniw M, Erb HN. Evaluation of four 2-dimensional echocardiographic methods of assessing left atrial size in dogs. *J Vet Intern Med*. 2000;14:429–435.
30. Plumb DC. Conversion of kg to m^2. In: D.C. Plumb, ed. *Plumb's Veterinary Drug Handbook (Pocket 7th Edition)*. Ames, IA: Wiley-Blackwell; 2011:1524.
31. Cerqueira MD, Weissman NJ, Dilsizian V, Jacobs AK, Kaul S, Laskey WK, Pennell DJ, Rumberger JA, Ryan T, Verani MS; American Heart Association Writing Group on Myocardial Segmentation and Registration for Cardiac Imaging. Standardized myocardial segmentation and nomenclature for tomographic imaging of the heart. A statement for healthcare professionals from the Cardiac Imaging Committee of the Council on Clinical Cardiology of the American Heart Association. *Circulation*. 2002;105:539–542.
32. Durrleman S, Simon R. Flexible regression models with cubic splines. *Stat Med*. 1989;8:551–561.
33. Reinsch CH. Smoothing by spline functions. *Numer Math*. 1967;10:177–183.
34. Soslow JH, Xu M, Slaughter JC, Stanley M, Crum K, Markham LW, Parra DA. Evaluation of echocardiographic measures of left ventricular function in patients with Duchenne muscular dystrophy: assessment of reproducibility and comparison to cardiac magnetic resonance imaging. *J Am Soc Echocardiogr*. 2016;29:983–991.
35. Ergul Y, Ekici B, Nisli K, Tatli B, Binboga F, Acar G, Ozmen M, Omeroglu RE. Evaluation of the North Star Ambulatory Assessment scale and cardiac abnormalities in ambulant boys with Duchenne muscular dystrophy. *J Paediatr Child Health*. 2012;48:610–616.
36. Spurney CF, McCaffrey FM, Cnaan A, Morgenroth LP, Ghelani SJ, Gordish-Dressman H, Arrieta A, Connolly AM, Lotze TE, McDonald CM, Leshner RT, Clemens PR. Feasibility and reproducibility of echocardiographic measures in children with muscular dystrophies. *J Am Soc Echocardiogr*. 2015;28:999–1008.
37. Dukes-McEwan J, Borgarelli M, Tidholm A, Vollmar AC, Häggström J. Proposed guidelines for the diagnosis of canine idiopathic dilated cardiomyopathy. *J Vet Cardiol*. 2003;5:7–19.
38. Morrison SA, Moise NS, Scarlett J, Mohammed H, Yeager AE. Effect of breed and body weight on echocardiographic values in four breeds of dogs of differing somatotype. *J Vet Intern Med*. 1992;6:220–224.
39. Dalal PG, Corner A, Chin C, Wood C, Razavi R. Comparison of the cardiovascular effects of isoflurane and sevoflurane as measured by magnetic resonance imaging in children with congenital heart disease. *J Clin Anesth*. 2008;20:40–44.
40. Hettrick DA, Pagel PS, Warltier DC. Desflurane, sevoflurane, and isoflurane impair canine left ventricular-arterial coupling and mechanical efficiency. *Anesthesiology*. 1996;85:403–413.
41. Kornegay JN, Bogan DJ, Bogan JR, Childers MK, Cundiff DD, Petroski GF, Schueler RO. Contraction force generated by tarsal joint flexion and extension in dogs with golden retriever muscular dystrophy. *J Neurol Sci*. 1999;166:115–121.
42. D'Amario D, Amodeo A, Adorisio R, Tiziano FD, Leone AM, Perri G, Bruno P, Massetti M, Ferlini A, Pane M, Niccoli G, Porto I, D'Angelo GA, Borovac JA,

Mercuri E, Crea F. A current approach to heart failure in Duchenne muscular dystrophy. *Heart*. 2017;103:1770–1779.

43. Kornegay JN. The golden retriever model of Duchenne muscular dystrophy. *Skelet Muscle*. 2017;7:9.
44. Kornegay JN, Spurney CF, Nghiem PP, Brinkmeyer-Langford CL, Hoffman EP, Nagaraju K. Pharmacologic management of Duchenne muscular dystrophy: target identification and preclinical trials. *ILAR J*. 2014;55:119–149.
45. Ryan TD, Taylor MD, Mazur W, Cripe LH, Pratt J, King EC, Lao K, Grenier MA, Jefferies JL, Benson DW, Hor KN. Abnormal circumferential strain is present in young Duchenne muscular dystrophy patients. *Pediatr Cardiol*. 2013;34:1159–1165.
46. Taqatqa A, Bokowski J, Al-Kubaisi M, Khalil A, Miranda C, Alaksham H, Fughhi I, Kenny D, Diab KA. The use of speckle tracking echocardiography for early detection of myocardial dysfunction in patients with Duchenne muscular dystrophy. *Pediatr Cardiol*. 2016;37:1422–1428.
47. Jo WH, Eun LY, Jung JW, Choi JY, Gang SW. Early marker of myocardial deformation in children with Duchenne muscular dystrophy assessed using echocardiographic myocardial strain analysis. *Yonsei Med J*. 2016;57:900–904.
48. Amedro P, Vincenti M, De La Villeon G, Lavastre K, Barrea C, Guillaumont S, Bredy C, Gamon L, Meli AC, Cazorla O, Fauconnier J, Meyer P, Rivier F, Adda J, Mura T, Lacampagne A. Speckle-tracking echocardiography in children with Duchenne muscular dystrophy: a prospective multicenter controlled cross-sectional study. *J Am Soc Echocardiogr*. 2019;32:412–422.
49. Serri K, Reant P, Lafitte M, Berhouet M, Le Bouffos V, Roudaut R, Lafitte S. Global and regional myocardial function quantification by two-dimensional strain: application in hypertrophic cardiomyopathy. *J Am Coll Cardiol*. 2006;47:1175–1181.
50. Arunamata A, Stringer J, Balasubramanian S, Tacy TA, Silverman NH, Punn R. Cardiac segmental strain analysis in pediatric left ventricular noncompaction cardiomyopathy. *J Am Soc Echocardiogr*. 2019;32:763–773.e1.
51. Kostakou PM, Kostopoulos VS, Tryfou ES, Giannaris VD, Rodis IE, Olympios CD, Kouris NT. Subclinical left ventricular dysfunction and correlation with regional strain analysis in myocarditis with normal ejection fraction. A new diagnostic criterion. *Int J Cardiol*. 2018;259:116–121.
52. Thavendiranathan P, Poulin F, Lim KD, Plana JC, Woo A, Marwick TH. Use of myocardial strain imaging by echocardiography for the early detection of cardiotoxicity in patients during and after cancer chemotherapy: a systematic review. *J Am Coll Cardiol*. 2014;63:2751–2768.
53. Bogarapu S, Puchalski MD, Everitt MD, Williams RV, Weng HY, Menon SC. Novel cardiac magnetic resonance feature tracking (CMR-FT) analysis for detection of myocardial fibrosis in pediatric hypertrophic cardiomyopathy. *Pediatr Cardiol*. 2016;37:663–673.
54. Weigand J, Nielsen JC, Sengupta PP, Sanz J, Srivastava S, Uppu S. Feature tracking-derived peak systolic strain compared to late gadolinium enhancement in troponin-positive myocarditis: a case-control study. *Pediatr Cardiol*. 2016;37:696–703.
55. Dusenbery SM, Lunze FI, Jerosch-Herold M, Geva T, Newburger JW, Colan SD, Powell AJ. Left ventricular strain and myocardial fibrosis in congenital aortic stenosis. *Am J Cardiol*. 2015;116:1257–1262.
56. Markham LW, Michelfelder EC, Border WL, Khoury PR, Spicer RL, Wong BL, Benson DW, Cripe LH. Abnormalities of diastolic function precede dilated cardiomyopathy associated with Duchenne muscular dystrophy. *J Am Soc Echocardiogr*. 2006;19:865–871.
57. Karamitsos TD, Francis JM, Myerson S, Selvanayagam JB, Neubauer S. The role of cardiovascular magnetic resonance imaging in heart failure. *J Am Coll Cardiol*. 2009;54:1407–1424.
58. Siegel B, Olivieri L, Gordish-Dressman H, Spurney CF. Myocardial strain using cardiac MR feature tracking and speckle tracking echocardiography in Duchenne muscular dystrophy patients. *Pediatr Cardiol*. 2018;39:478–483.
59. Nakamura M, Sadoshima J. Mechanisms of physiological and pathological cardiac hypertrophy. *Nat Rev Cardiol*. 2018;15:387–407.
60. Hor KN, Taylor MD, Al-Khalidi HR, Cripe LH, Raman SV, Jefferies JL, O'Donnell R, Benson DW, Mazur W. Prevalence and distribution of late gadolinium enhancement in a large population of patients with Duchenne muscular dystrophy: effect of age and left ventricular systolic function. *J Cardiovasc Magn Reson*. 2013;15:107.
61. Restrepo CS, Tavakoli S, Marmol-Velez A. Contrast-enhanced cardiac magnetic resonance imaging. *Magn Reson Imaging Clin N Am*. 2012;20:739–760.
62. Puchalski MD, Williams RV, Askovich B, Sower CT, Hor KH, Su JT, Pack N, Dibella E, Gottliebson WM. Late gadolinium enhancement: precursor to cardiomyopathy in Duchenne muscular dystrophy? *Int J Cardiovasc Imaging*. 2009;25:57–63.
63. Kellman P, Hernando D, Arai AE. Myocardial fat imaging. *Curr Cardiovasc Imaging Rep*. 2010;3:83–91.
64. Heymsfield SB, McNish T, Perkins JV, Felner JM. Sequence of cardiac changes in Duchenne muscular dystrophy. *Am Heart J*. 1978;95:283–294.
65. Posner AD, Soslow JH, Burnette WB, Bian A, Shintani A, Sawyer DB, Markham LW. The correlation of skeletal and cardiac muscle dysfunction in Duchenne muscular dystrophy. *J Neuromuscul Dis*. 2016;3:91–99.
66. Crisp A, Yin H, Goyenvalle A, Betts C, Moulton HM, Seow Y, Babbs A, Merritt T, Saleh AF, Gait MJ, Stuckey DJ, Clarke K, Davies KE, Wood MJ. Diaphragm rescue alone prevents heart dysfunction in dystrophic mice. *Hum Mol Genet*. 2011;20:413–421.
67. Townsend D, Yasuda S, Li S, Chamberlain JS, Metzger JM. Emergent dilated cardiomyopathy caused by targeted repair of dystrophic skeletal muscle. *Mol Ther*. 2008;16:832–835.
68. Wasala NB, Bostick B, Yue Y, Duan D. Exclusive skeletal muscle correction does not modulate dystrophic heart disease in the aged mdx model of Duchenne cardiomyopathy. *Hum Mol Genet*. 2013;22:2634–2641.
69. Barthelemy I, Pinto-Mariz F, Yada E, Desquilbet L, Savino W, Silva-Barbosa SD, Faussat AM, Mouly V, Voit T, Blot S, Butler-Browne G. Predictive markers of clinical outcome in the GRMD dog model of Duchenne muscular dystrophy. *Dis Model Mech*. 2014;7:1253–1261.
70. Vieira NM, Elvers I, Alexander MS, Moreira YB, Eran A, Gomes JP, Marshall JL, Karlsson EK, Verjovski-Almeida S, Lindblad-Toh K, Kunkel LM, Zatz M. Jagged 1 rescues the Duchenne muscular dystrophy phenotype. *Cell*. 2015;163:1204–1213.
71. Su JB, Cazorla O, Blot S, Blanchard-Gutton N, Ait Mou Y, Barthelemy I, Sambin L, Sampedrano CC, Gouni V, Unterfinger Y, Aguilar P, Thibaud JL, Bize A, Pouchelon JL, Dabire H, Ghaleb B, Berdeaux A, Chetboul V, Lacampagne A, Hittinger L. Bradykinin restores left ventricular function, sarcomeric protein phosphorylation, and e/nNOS levels in dogs with Duchenne muscular dystrophy cardiomyopathy. *Cardiovasc Res*. 2012;95:86–96.
72. Chetboul V, Carlos C, Blot S, Thibaud JL, Escriou C, Tissier R, Retortillo JL, Pouchelon JL. Tissue Doppler assessment of diastolic and systolic alterations of radial and longitudinal left ventricular motions in golden retrievers during the preclinical phase of cardiomyopathy associated with muscular dystrophy. *Am J Vet Res*. 2004;65:1335–1341.
73. Maruyama R, Echigoya Y, Caluseriu O, Aoki Y, Takeda S, Yokota T. Systemic delivery of morpholinos to skip multiple exons in a dog model of Duchenne muscular dystrophy. *Methods Mol Biol*. 2017;1565:201–213.
74. Le Guiner C, Servais L, Montus M, Larcher T, Fraysse B, Moullec S, Allais M, Francois V, Dutilleul M, Malerba A, Koo T, Thibaut JL, Matot B, Devaux M, Le Duff J, Deschamps JY, Barthelemy I, Blot S, Testault I, Wahbi K, Ederhy S, Martin S, Veron P, Georger C, Athanasopoulos T, Masurier C, Mingozzi F, Carlier P, Gjata B, Hogrel JY, Adjali O, Mavilio F, Voit T, Moullier P, Dickson G. Long-term microdystrophin gene therapy is effective in a canine model of Duchenne muscular dystrophy. *Nat Commun*. 2017;8:16105.
75. Barthelemy F, Wein N. Personalized gene and cell therapy for Duchenne muscular dystrophy. *Neuromuscul Disord*. 2018;28:803–824.

SUPPLEMENTAL MATERIAL

Data S1. Supplemental Methods

Normalization of echocardiographic M-mode results

In this study, we normalized our M-mode results, including IVSd, LVIDd, LVPWd, IVSs, LVIDs, LVPWs, LA and Ao diameter, for the dog's body mass using the method previously published by Cornell et al.[1]

$$\text{IVSd-n (cm/kg)} = \text{IVSd (cm)} / [\text{Body weight (kg)}]^{0.241}$$

$$\text{LVIDd-n (cm/kg)} = \text{LVIDd (cm)} / [\text{Body weight (kg)}]^{0.294}$$

$$\text{LVPWd-n (cm/kg)} = \text{LVPWd (cm)} / [\text{Body weight (kg)}]^{0.232}$$

$$\text{IVSs-n (cm/kg)} = \text{IVSs (cm)} / [\text{Body weight (kg)}]^{0.240}$$

$$\text{LVIDs-n (cm/kg)} = \text{LVIDs (cm)} / [\text{Body weight (kg)}]^{0.315}$$

$$\text{LVPWs-n (cm/kg)} = \text{LVPWs (cm)} / [\text{Body weight (kg)}]^{0.222}$$

$$\text{LA-n (cm/kg)} = \text{LA (cm)} / [\text{Body weight (kg)}]^{0.345}$$

$$\text{Ao-n (cm/kg)} = \text{Ao (cm)} / [\text{Body weight (kg)}]^{0.341}$$

IVSd indicates interventricular septum in diastole; LVIDd, left ventricular internal diameter in diastole; LVPWd, left ventricular posterior wall in diastole; IVSs, interventricular septum in systole; LVIDs, left ventricular internal diameter in systole; LVPWs, left ventricular posterior wall in systole; LA, left atrial diameter; Ao, aortic diameter; -n, normalization values.

Supplemental Reference:

1. Cornell CC, Kittleson MD, Della Torre P, Haggstrom J, Lombard CW, Pedersen HD, Vollmar A, Wey A. Allometric scaling of m-mode cardiac measurements in normal adult dogs. *J Vet Intern Med.* 2004;18:311-321.

Body surface area normalization of echocardiographic and CMR results

To accommodate for the differences in the dogs' body sizes, we normalized several echocardiographic and CMR parameters for body surface area (BSA).

BSA in $m^2 = 10.1 \times (\text{weight in grams})^{2/3} / 10000$

LVEDVI (mL/m^2) = LVEDV (mL) / BSA (m^2)

LVESVI (mL/m^2) = LVESV (mL) / BSA (m^2)

SV Index (mL/m^2) = SV (mL) / BSA (m^2)

Myo Mass Index (g/m^2) = Myo Mass (g) / BSA (m^2)

CMR indicates cardiac magnetic resonance imaging; LVEDVI, left ventricular end-diastolic volume index; LVESVI, left ventricular end-systolic volume index; SV index, stroke volume index; Myo Mass Index, myocardial mass index.

The scoring method for semi-quantitative LGE analysis.

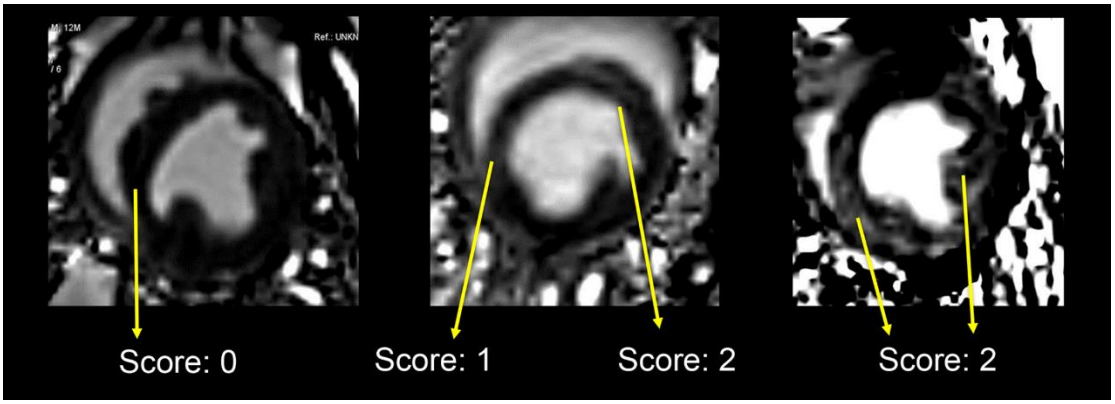

Non-enhancing segments shown as dark/black were scored as 0. Those with intermediate enhancement shown as grey were scored as 1. Areas of marked enhancement shown as bright/white were scored as 2. LGE indicates late gadolinium enhancement.

Table S1. Dogs assessed with echocardiography and CMR

Animal Number	Sex	Age	Equipment
Echocardiography – Single Time Point			
11 dogs	7 males	17–86 months	GE Vivid 9
	4 females		
8 dogs	7 males	21–35 months	Siemens Antares
	1 female		
Echocardiography – Longitudinal Study			
10 dogs	8 males	10 or 22 months†	Siemens Antares
	2 females		
CMR – Single Time Point			
17 dogs	9 males	9–77 months	Siemens 3T MRI
	8 females		

† Age at dog's first echocardiographic scan. Six males were aged 22 months. Two males and 2 females were aged 10 months.

CMR indicates cardiac magnetic resonance imaging.

Table S2. Body weight, body surface area, and echocardiographic variables across age groups of the single time point study

		<30m old **Median (Min–Max)** **N=7**	**30–45m old** **Median (Min–Max)** **N=7**	**>45m old** **Median (Min–Max)** **N=5**
Age (month)		21 (17–25)	33 (30–41)	76 (46–86)
Body Weight (kg)		17.4 (12.5–21.8)	18.1 (14.9–27.7)	18.4 (13.8–24.8)
Body Surface Area (m^2)		0.68 (0.54–0.79)	0.70 (0.61–0.93)	0.70 (0.58–0.86)
Echocardiography				
2D	LVEDV (mL)	32 (15–44)	32 (21–62)	61*† (49–87)
	LVESV (mL)	13 (5–18)	13 (9–37)	33* (31–71)
	SV (mL)	20 (10–29)	19 (12–25)	20 (16–28)
	EF (%)	60 (54–65)	54 (39–71)	35** (19–45)
	LVEDVI§ (mL/m^2)	47.48 (27.55–56.56)	44.71 (30.14–101.30)	84.25*† (67.19–124.85)
	LVESVI§ (mL/m^2)	18.50 (9.18–25.95)	17.90 (12.92–60.45)	53.30*† (38.42–101.89)
	SV Index§ (mL/m^2)	28.03 (18.37–36.16)	24.59 (17.22–40.85)	28.41 (22.96–32.60)
M-mode	Heart Rate (bpm)	148 (90–156)	112 (82–154)	123 (109–162)
	IVSd (cm)	0.7 (0.6–1.1)	0.9 (0.6–1.0)	0.9 (0.7–1.1)
	LVIDd (cm)	3.5 (2.4–4.0)	3.8 (2.2–4.1)	4.5* (3.9–5.7)
	LVPWd (cm)	0.8 (0.6–1.1)	0.9 (0.6–1.1)	0.8 (0.7–1.0)
	IVSs (cm)	1.0 (0.9–1.4)	1.1 (0.9–1.2)	0.9 (0.7–1.5)
	LVIDs (cm)	2.2 (1.5–3.1)	2.6 (1.4–3.5)	3.4** (3.2–5.2)
	LVPWs (cm)	1.1 (0.8–1.5)	1.3 (0.9–1.5)	1.2 (1.0–1.3)
	FS (%)	36 (23–39)	33 (14–36)	18* (9–24)
	IVSd-n§ (cm/kg)	0.38 (0.32–0.52)	0.40 (0.30–0.52)	0.545 (0.35–0.58)
	LVIDd-n§ (cm/kg)	1.49 (1.14–1.72)	1.54 (0.94–1.85)	1.94* (1.58–2.43)
	LVPWd-n§ (cm/kg)	0.39 (0.32–0.51)	0.46 (0.28–0.59)	0.44 (0.36–0.47)

	IVSs-n§ (cm/kg)	0.55 (0.43–0.69)	0.53 (0.44–0.58)	0.48 (0.35–0.69)
	LVIDs-n§ (cm/kg)	0.88 (0.68–1.25)	1.02 (0.56–1.49)	1.40* (1.21–2.09)
	LVPWs-n§ (cm/kg)	0.58 (0.44–0.79)	0.62 (0.45–0.80)	0.61 (0.53–0.64)
Doppler	AV Vmax (m/s)	1.12 (0.84–1.59)	1.05 (0.82–1.35)	1.39 (0.74–1.68)
	MV E Velocity (m/s)	0.75 (0.55–0.90)	0.86 (0.61–1.00)	0.90 (0.58–1.01)
	MV A Velocity (m/s)	0.47 (0.38–0.59)	0.35 (0.25–0.68)	0.71† (0.55–0.97)
	E/A Ratio	1.52 (1.35–1.95)	2.23 (1.50–3.32)	1.38† (0.60–1.66)
TDI	E/Em (LV Lateral)	5.63 (4.05–7.00)	6.50 (5.38–9.89)	9.38* (6.31–14.50)
	E/Em (LV Septal)	7.70 (6.36–8.40)	9.495* (8.50–12.71)	11.25* (8.42–11.60)
		<30m old Median (Min–Max) (N=2)‡	**30–45m old Median (Min–Max) (N=4)‡**	**>45m old Median (Min–Max) (N=5)‡**
2D	LA/Ao	0.915 (0.82–1.01)	1.025 (0.95–1.70)	1.24 (1.06–2.09)
Doppler	IVRT (ms)	57 (53–61)	69 (55–93)	69 (53–106)
Strain	Circ Strain (%)	-24.24 (-25.42 to -23.06)	-15.93 (-24.97 to -11.27)	-10.12 (-19.50 to -3.89)
	Circ Strain Rate (1/s)	-2.195 (-2.35 to -2.04)	-1.36 (-2.07 to -0.95)	-0.82 (-1.83 to -0.38)

‡ Data were only collected from 11 dogs (n=2 for <30m; n=4 for 30–45m; n=5 for >45m) scanned with the GE Vivid 9 ultrasound machine.

§ Values after normalizations. LVEDVI, LVESVI, and SV Index are the values after body surface area normalization. IVSd-n, LVIDd-n, LVPWd-n, IVSs-n, LVIDs-n, LVPWs-n are the values after body mass normalization.

LVEDV indicates left ventricular end-diastolic volume; LVESV, left ventricular end-systolic volume; SV, stroke volume; EF, ejection fraction; LVEDVI, left ventricular end-diastolic volume index; LVESVI, left ventricular end-systolic volume index; SV Index, stroke volume index; IVSd

interventricular septum in diastole; LVIDd, left ventricular internal diameter in diastole; LVPWd, left ventricular posterior wall in diastole; IVSs, interventricular septum in systole; LVIDs, left ventricular internal diameter in systole; LVPWs, Left ventricular posterior wall in systole; FS, fractional shortening; -n, normalization values; AV Vmax, maximal velocity at aortic valve; MV E Velocity, mitral valve E wave velocity; MV A Velocity, mitral valve A wave velocity; E/A Ratio, mitral valve E wave to A wave ratio; TDI, tissue Doppler imaging; E/Em (LV Lateral), ratio of mitral valve E wave to TDI Em wave at left ventricular lateral wall; E/Em (LV Septal), ratio of mitral valve E wave to TDI Em wave at left ventricular septal wall; LA/Ao, Left atrial to aortic root ratio; IVRT, isovolumic relaxation time; Circ Strain, circumferential strain; Circ Strain Rate, circumferential strain rate.

* Median differed (P<0.05) from <30 month group.

† Median differed (P<0.05) from 30–45 month group.

** Median differed (P<0.01) from <30 month group.

Table S3. Segmental and average circumferential strain and strain rate changes in longitudinal study

	LV Segment	1st Scan Median (Min–Max)	2nd Scan Median (Min–Max)	*P* Value†
10 month group (10 to 22 months; n=4)				
Circumferential Strain (%)				
	Anterior	-13.94 (-17.48 to -12.02)	-20.08 (-29.40 to -10.98)	0.25
	Anteroseptal	-22.29 (-26.96 to -17.51)	-23.27 (-28.86 to -16.30)	0.63
	Inferoseptal	-18.215 (-23.05 to -15.23)	-20.425 (-25.06 to -14.17)	1.00
	Inferior	-14.41 (-27.64 to -12.77)	-16.94 (-20.94 to -8.95)	0.88
	Inferolateral	-20.14 (-22.54 to -16.88)	-16.77 (-24.50 to -9.07)	0.38
	Anterolateral	-17.24 (-20.31 to -16.15)	-16.34 (-21.91 to -11.86)	0.88
	Average	-17.39 (-22.57 to -16.05)	-17.90 (-24.32 to -14.83)	0.88
Circumferential Strain Rate (1/s)				
	Anterior	-1.46 (-1.82 to -0.97)	-1.63 (-2.66 to -0.99)	0.63
	Anteroseptal	-2.09 (-2.78 to -1.32)	-2.015 (-2.64 to -1.53)	0.88
	Inferoseptal	-1.71 (-2.47 to -1.35)	-1.865 (-2.89 to -1.14)	0.63
	Inferior	-1.36 (-3.12 to -1.15)	-1.66 (-2.23 to -0.84)	0.63
	Inferolateral	-2.09 (-2.85 to -1.44)	-1.79 (-2.10 to -0.83)	0.13
	Anterolateral	-1.93 (-2.16 to -1.58)	-1.43 (-1.88 to -1.15)	0.13
	Average	-1.815 (-2.45 to -1.30)	-1.835 (-2.07 to -1.20)	0.63
22 month group (22 to 34 months; n=6)				
Circumferential Strain (%)				
	Anterior	-12.51 (-18.80 to -5.90)	-12.62 (-20.73 to -7.50)	0.69
	Anteroseptal	-19.83 (-30.94 to -15.25)	-16.81 (-20.35 to -10.73)	0.03*
	Inferoseptal	-21.13 (-31.83 to -17.38)	-16.14 (-21.86 to -4.30)	0.06
	Inferior	-16.42 (-18.48 to -9.88)	-8.805 (-16.34 to -6.12)	0.03*

	Inferolateral	-21.14 (-24.12 to -9.78)	-13.07 (-20.71 to -10.18)	0.09
	Anterolateral	-19.02 (-27.98 to -8.30)	-16.63 (-24.19 to -14.16)	0.44
	Average	-19.07 (-24.30 to -12.71)	-14.715 (-18.09 to -10.50)	0.03*
Circumferential Strain Rate (1/s)				
	Anterior	-0.85 (-1.44 to -0.28)	-1.00 (-1.50 to -0.72)	0.44
	Anteroseptal	-1.54 (-2.75 to -0.30)	-1.375 (-1.47 to -1.03)	0.84
	Inferoseptal	-1.51 (-2.67 to -0.42)	-1.28 (-1.83 to -0.76)	0.56
	Inferior	-1.26 (-1.74 to -0.76)	-0.80 (-1.35 to -0.71)	0.22
	Inferolateral	-1.23 (-2.70 to -0.87)	-1.22 (-1.91 to -0.78)	0.44
	Anterolateral	-1.18 (-3.41 to -0.55)	-1.36 (-2.15 to -1.22)	0.84
	Average	-1.225 (-2.28 to -0.41)	-1.18 (-1.51 to -1.00)	0.84

LV indicates left ventricle.

† Wilcoxon signed rank test was used. * $P<0.05$.

Table S4. Body weight, body surface area, and CMR variables across age groups

	<30m old **Median (Min–Max)** **N=8**	**30–45m old** **Median (Min–Max)** **N=4**	**>45m old** **Median (Min–Max)** **N=2**
Age (month)	21 (9–22)	32.5 (30–41)	61.5 (46–77)
Body Weight† (kg)	15.21 (12.51–17.52)	17.87 (17.12–27.73)	19.97 (18.12–21.82)
Body Surface Area† (m^2)	0.62 (0.54–0.68)	0.69 (0.67–0.92)	0.74 (0.69–0.78)
CMR Analysis			
Heart Rate (bpm)	136 (121–145)	133.5 (98–144)	134.5 (133–136)
EF† (%)	50.35 (33.3–65.4)	35.95 (31.0–55.9)	12.35 (9.8–14.9)
LVEDV (mL)	32.3 (22.6–49.8)	45.7 (44.6–50.0)	95.6* (82.6–108.6)
LVESV (mL)	16.1 (7.9–33.2)	30.75 (19.8–31.0)	84.1* (70.3–97.9)
SV (mL)	16.55 (14.1–17.8)	17.4 (13.8–25.1)	11.5 (10.7–12.3)
Myo Mass (g)	43.35 (26.9–53.0)	63.8 (60.5–70.0)	75.8* (72.6–79.0)
BSA Normalization			
LVEDVI† (mL/m^2)	52.58 (40.01–73.71)	66.21 (48.20–74.52)	130.28 (104.71–155.84)
LVESVI (mL/m^2)	26.22 (14.03–49.10)	39.08 (28.41–46.20)	114.80 (89.12–140.49)
SV Index (mL/m^2)	26.36 (21.70–28.21)	25.71 (14.91–36.02)	15.47 (15.35–15.59)
Myo Mass Index† (g/m^2)	68.97 (43.37–88.49)	93.27 (65.38–102.34)	102.17 (100.15–104.18)

CMR indicates cardiac magnetic resonance imaging; EF, ejection fraction; LVEDV, left ventricular end-diastolic volume; LVESV, left ventricular end-systolic volume; SV, stroke volume; Myo Mass, myocardial mass; BSA, body surface area; LVEDVI, left ventricular end-diastolic volume index; LVESVI, left ventricular end-systolic volume index; SV Index, stroke volume index; Myo Mass Index, myocardial mass index.

* Median differed ($P<0.05$) from <30 month group.

† Statistical significance ($P<0.05$) was found with the Kruskal-Wallis test but not with Dunn's test.